91602
new 82-10 LEGAL NOTICE

This report was prepared by Ontario Hydro and, while effort has been made to assure the accuracy and applicability of the material contained herein, neither Ontario Hydro nor any person acting on its behalf:

(a) makes any warranty, express or implied with respect to the use of any information, apparatus, method or process disclosed in this report or that such use may not infringe privately owned rights; or

(b) assumes any liabilities with respect to the use of, or for damages resulting from the use of, any information, apparatus, method or process disclosed in this report.

ontario hydro
research division

COMPLIMENTARY COPY
Please Credit Ontario Hydro Research if Reproduced in Whole or in Part

REACTOR OPERATING WASTE DISPOSAL PROGRAM
1989 PROGRESS REPORT

Report No 89-226-K

R. Dayal
Program Coordinator
H. Johnston
Hydrogeologist
Z. Zhou
Engineer
Rock Sciences Section
Civil Research Department

Abstract

This report presents the progress made to date in the Civil Research Department's Reactor Operating Waste Disposal Program. The research program is focusing on both the near- and far-field investigations relevant to the long-term isolation of C-14. Specifically, the near-field investigations involve evaluation of the source term for C-14 and the effectiveness of cement-based backfill materials for radiocarbon attenuation, whereas the far-field investigations are focusing on the behaviour and transport of C-14 in natural geologic materials. Work is also progressing on evaluation of concrete materials for high integrity containers for the storage/disposal of reactor operating waste. Evaluation of existing geochemical data, derived from the low-level waste disposal sites in the United States, is being conducted to establish the geochemical conditions and processes related to radionuclide mobility at these sites. Results obtained to-date in the various research projects are summarized and discussed, paying particular attention to their relevance to Ontario Hydro's reactor operating waste management program.

job	file	date	report no.
44-204/44-205,44-203 44-528, 44-318	841.2	October 27, 1989	89-226-K

TABLE OF CONTENTS

		Page
1.0	INTRODUCTION	1
2.0	DESCRIPTION AND CURRENT STATUS OF THE PROGRAM	2
2.1	Cement-Based Backfill Materials Evaluation	2
2.2	Source Term Evaluation for C-14	19
2.3	Concrete Materials for High Integrity Containers	22
2.4	Transport of C-14 in Unsaturated Geologic Materials	36
2.5	Recrystallization Uptake of C-14 on Carbonate Minerals	45
2.6	Evaluation of Geochemical Data from the U.S. Low-Level Waste Disposal Sites	47
2.61	Exchange and Transport of $^{14}CO_2$ in the Unsaturated Zone at the Sheffield Radioactive Waste Disposal Site	48
2.62	Source Term Composition of Trench Leachates from the Maxey Flats Radioactive Waste Disposal Site	49
2.63	Sediment Core Radionuclide Data from the Barnwell Radioactive Disposal Site	56
3.0	CONCLUSIONS	56
3.1	Cement-Based Backfill Materials Evaluation	56
3.2	Source Term Evaluation for C-14	57
3.3	Concrete Materials for High Integrity Containers	58
3.4	Transport of C-14 in Unsaturated Geologic Materials	58
3.5	Recrystallization Uptake of C-14 on Carbonate Minerals	59
3.6	Evaluation of Geochemical Data from the U.S. Low-Level Radioactive Waste Disposal Sites	59
4.0	ACKNOWLEDGMENTS	62
REFERENCES		63
APPENDIX I		65
DISTRIBUTION		last page

LIST OF TABLES

Table		Page
1	Material Compositions and Mix Proportions	4
2	Factors Affecting Grout Carbonation	6
3	Carbonation Capacities for the Various Grout Test Materials	7
4	Changes Induced in Material Transport Properties as a Result of Carbonation	16
5	Effect of Flow Rate on C-14 Leach Rates	20
6	Test Mixes and Mix Formulations	24
7	Chemical Compositions of SF, SRPC and BFS	24
8	Final Compositions of the Test Mixes	25
9	Chemical Composition of BNPD Groundwater	26
10	Gas Permeability and Porosity Data on Test Materials	26
11	Changes in Mass of Test Specimen Following Leaching	30
12	Dissolution and Precipitation Reactions Occurring in Concrete/Water Systems	33
13	Calculated Distribution Coefficients	39
14	Measured $^{14}CO_2(g)$ Diffusion Coefficients	41
15	Chemical Composition of Trench Leachate 19s from the Maxey Flats LLW Disposal Site	52

LIST OF FIGURES

Figure		Page
1	% CO_2 uptake versus time for a sample of solid grout.	8
2	% CO_2 uptake versus time for a sample of solid grout. Vertical arrows indicate times at which the sample cell was dismantled and the sample dried under vacuum.	8
3	The effect of drying on the rate of carbonation.	10
4	% CO_2 uptake versus time for a sample vacuum dried for two weeks and subjected to a p_{CO_2} of 400 psi.	10
5	% CO_2 uptake for a sample of powdered grout.	11
6	Simulation of progressive carbonation reaction in a grout/water system, showing the predominant mineral phases exerting control on the evolving solution chemistry.	12
7	Nitrogen and carbon dioxide pressure decay tests show the effect of successive carbonations on material permeability.	14
8	Nitrogen pressure decay curves for test specimen 13901 before and after carbonation, showing an exponential relationship and a decrease in permeability following carbonation.	15
9	Constant pressure flow tests on specimen 13901, indicating a reduction in permeability following carbonation.	15
10	Photomicrograph showing a highly carbonated paste.	17
11	A close-up of photomicrograph in Figure 10, showing reaction rims of calcitic material around silicate grains, as well as a highly carbonated cement paste.	17
12	Photomicrograph showing microcracks filled in with highly birefringent calcitic material, as well as reaction rims around silicate grains and a relatively less carbonated cement paste.	18
13	Photomicrograph showing cement paste with a granular, mottled texture, completely devoid of any carbonation features.	18
14	Ca^{2+} - pH relationship showing calcite solubility as affected by pH for two concentration levels of DIC.	21
15	Cumulative fractional release (CFR) of C-14 versus time under high flow leaching conditions.	23

LIST OF FIGURES

Figure		Page
16	The evolution of average pH within a cement-based repository of radius 20 m.	23
17	Cumulative fractional releases of calcium and silica for the test mixes (13871, 13872, 13873, 13874) subjected to deionized water leaching under dynamic conditions.	27
18	Leachate pH versus time for the test mixes (13871, 13872, 13873, 13874) subjected to deionized water leaching under dynamic conditions.	28
19	Light micrographs of leached specimens showing development of a calcitic reaction rim at the periphery and around the interconnected vesicles in the test specimen.	31
20	Leaching-induced changes in microstructural properties of the exterior radial zone of test specimen (1,3). The inner core is represented by 2, while the shaded areas represent unleached specimen.	32
21	Changes in mineral saturation indices with time for the four test mixes subjected to deionized water leaching under static conditions.	34
22	Cumulative fractional releases of calcium and silica for test specimen 13871 subjected to both static and dynamic leaching conditions with deionized water and BNPD groundwater as leachants.	35
23	Schematic of batch exchange system.	37
24	C-14 uptake kinetics; (a) 0.1% CO_2; (b) 1% CO_2; (c) 10% CO_2.	38
25	Effect of gas-liquid volume ratio on K1 values.	40
26	Measured $^{14}CO_2$ concentration profiles - 5% gravimetric moisture content, 1% pCO_2.	42
27	Effect of isotopic exchange on measured diffusion coefficients.	43
28	Effect of isotope exchange on gaseous C-14 migration.	44
29	Comparison of measured to calculated diffusion coefficients.	44
30	Reaction vessel for long-term C-14 equilibrium batch tests.	46
31	Distribution coefficients (Kd) for C-14 versus time, based on equilibrium batch tests for calcite.	47
32	The Eh-pH relationships for leachates 27 and 19s depicting different reaction paths and progress during oxidation.	51

LIST OF FIGURES

Figure		Page
33	Predicted (solid line) and observed (•) changes in anoxic leachate chemistry (19s) with increasing degree of oxidation.	53
34	Changes in carbonate mineral saturation indices with progressive oxidation of anoxic leachate 19s.	54
35	The Eh-pH relationship for leachate 19s reaction path and progress during oxidation.	55

ontario hydro
research division

To Mr. D.W. Souther
Manager
Nuclear Engineering Dept.
Design & Development Div - Gen., H10A1

Attention: Mr. P.D. Stevens-Guille/Mr. P. Mitchell

REACTOR OPERATING WASTE DISPOSAL PROGRAM
1989 PROGRESS REPORT

1.0 INTRODUCTION

The development of the nuclear power industry in Ontario has resulted in an increasing accumulation of low- to medium-level radioactive wastes. The principal source of radioactivity in solid reactor wastes is concentrated on the ion-exchange resins used in the purification systems of the heavy water moderator, reactor coolant, and spent-fuel bay systems. Spent moderator ion-exchange resins contain major amounts of neutron-activation products such as Co-60, Fe-59, and Cr-51. In addition, significant quantities of C-14, which is produced from the neutron activation of O-17 in the moderator heavy water, accumulate on the ion-exchange resin (1). In the analysis of moderator resins from Bruce GS-A for example, C-14 constitutes ~84% of the total radionuclide activity (2).

Most of the options currently being considered for the long-term management of these wastes involve storage in geological formations or in engineered structures at ground surface. Thus, an important consideration in the environmental assessment of waste management sites is the possibility of the escape of radionuclides from these facilities and the subsequent transport to the biosphere.

The Nuclear Engineering Department at Ontario Hydro is conducting a Research and Development Program to develop a data base needed for formulating a strategy for the long-term management of these wastes (3,4). This is particularly important in view of the fact that storage to de minimis is not a valid option for management of C-14, a long-lived isotope ($t^{1/2}$ = 5730 years) present in significant amounts in CANDU reactor operating wastes. Furthermore, the relatively conservative migration behaviour of $H^{14}CO_3^-$ in the natural geologic environment points to the importance of the use of engineered barriers in providing the desired containment for time periods commensurate with its half-life.

Giving no credit to the attenuation properties of engineered barriers, performance assessment modeling using simple radiological models has shown the public dose from a hypothetical low-level waste site located at the Bruce Nuclear Power Development (BNPD) would be due primarily to C-14 exposure (5). More recent modeling efforts, however, are considering the containment properties and the lag time involved in the leaching of C-14 from a cement-based waste form (6).

In view of these considerations, a major component of the Nuclear Engineering Department Research and Development Program pertains to research for long-term management for C-14 (4). As part of this overall R & D program, the Civil Research Department's Reactor Operating Waste Disposal Program is focusing on both the near- and far-field investigations relevant to the long-term isolation of C-14. Specifically, the near-field investigations involve evaluation of the source term for C-14 and the effectiveness of cement-based backfill materials for radiocarbon attenuation, whereas the far-field investigations are focusing on the behaviour and transport of C-14 in natural geologic materials under both saturated and unsaturated moisture conditions. Considering that very limited data is available in this important area, the research underway in the Civil Research Department is designed to provide a fundamental understanding of the processes controlling C-14 concentrations and mobility both in the near- and far-field environs of a repository.

Although the majority of the research effort pertains to C-14 isolation studies, work is also progressing on the evaluation of candidate concrete materials for high integrity containers for the storage/disposal of reactor operating waste, with particular reference to the IC-57 Inground Containers being considered by the Nuclear Engineering Department for the 200-year storage program. Another important aspect of the Reactor Operating Waste Disposal Program is the review and evaluation of existing geochemical data, derived from the low-level radioactive waste disposal sites in the United States, for the purpose of establishing the geochemical conditions and processes related to source term characteristics and radionuclide mobility at the sites. The data are being evaluated in the context of their relevance to Ontario Hydro's Reactor Operating Waste Management Program.

2.0 DESCRIPTION AND CURRENT STATUS OF THE PROGRAM

In this report, we have outlined the research performed in the various projects in the Reactor Operating Waste Disposal Program. Results obtained to-date for each project are summarized and discussed, paying particular attention to their relevance to Ontario Hydro's reactor operating waste management program.

2.1 CEMENT-BASED BACKFILL MATERIALS EVALUATION

Objective: The main purpose of the study is to assess the effectiveness of cement-based backfill materials as a geochemical sink for radiocarbon. Containment of C-14 by engineered barriers would contribute greatly to its long-term management requirements, given its long half life, volatile nature, and high mobility in the natural geologic environment.

Work Plan: To meet the above objective, the following work has been completed or is in progress on selected grout materials.

- Determination of the total carbonation capacities of selected grout formulations
- Identification of the relevant processes by which carbonation occurs
- Identification of carbonation-induced changes in material properties
- Evaluation of the effects of carbonation on long-term durability and performance of backfill
- Development of a model for radiocarbon reaction and transport in grout backfill

Description of Laboratory Work: As part of this research project, laboratory investigations have been underway at Ontario Hydro and the University of Waterloo to evaluate CO_2/grout interactions and their relevance to radiocarbon attenuation in cement-based grout materials (7,8,9,10,11). Laboratory tests performed at the University of Waterloo have focused primarily on the carbonation of cement paste (water/cement ratio = 0.40), emphasizing the mechanistic aspects of grout carbonation. Work at Ontario Hydro is focusing on evaluating a range of grout formulations of differing compositions (Table 1) to obtain a more generic data base on the carbonation properties of the test materials. As part of Ontario Hydro's research, a considerable amount of effort has also been directed at the identification of carbonation-induced changes in material properties affecting both the material transport characteristics and long-term durability.

The following section summarizes the various types of laboratory tests that have been conducted in this research project to investigate specific aspects of grout carbonation.

A. Reaction-Controlled Carbonation Tests

Giving no credit to the matrix transport parameters, carbonation tests were performed on powdered grout specimens to accelerate the carbonation reaction, as well as to investigate reaction-controlled carbonate uptake kinetics, carbonation mechanisms, and total carbonation capacities. Specifically, three types of laboratory tests were conducted or are planned to study the various aspects of grout/carbonate interactions outlined below.

A.1. Powdered Grout/CO_2 Tests

- Carbonate Uptake Kinetics
- Total Carbonation Capacity
- Carbonation-Induced Changes in Grout Chemical and Minerological Composition

A.2 Powdered Grout/Water/CO_2 Tests

- Geochemical Evaluation of Water Chemistry with Progressive Carbonation
- Changing Mineralogical Controls on Evolving Water Chemistry
- Evolving Solid Reaction Products with Progressive Carbonation
- Stability of Carbonation End Products with Respect to Long-Term Durability of Grout

A.3 Powdered Grout/$^{14}CO_3^{2-}$ Tests

- Radiocarbon Uptake Capacity
- Radiocarbon Uptake Kinetics

Table 1. Material Compositions and Mix Proportions

Material (Mix No)	Mix Proportions[a]				Admixture[a]		w/c[b] Ratio
	Cement	Sand	Water	Fly Ash	Intrusion Aid	Melmet	
Cement Grout (13711)	21120	31680	8450	-	211	-	0.40
Cement Grout (13712)	14080	35200	7180	-	141	-	0.51
Cement Grout (13713)	21120	31680	8450	-	-	317	0.40
Cement Grout (13714)	14080	35200	6900	-	-	211	0.49
Cement-Fly Ash Grout (13715)	16896	31680	6760	4224	211	-	0.40
Cement-Fly Ash Grout (13716)	11264	35200	5520	2816	141	-	0.49

[a]All values are given in grams.

[b]w/c = water/cement ratio.

B. Reaction & Transport-Controlled Carbonation Tests

In order to simulate a more realistic repository situation, intact grout specimens were carbonated to investigate the effects of material transport properties, in particular, the carbonation-induced changes that are likely to occur, on the overall carbonation process. Specifically, the following tests have been performed or are planned on intact grout specimens to determine the nature and extent of carbonation under both diffusive and advective carbonating conditions.

B.1 Diffusion-Controlled CO_2/Grout Tests

- Nature and Extent of Carbonation
- Rate of Advance of Carbonation Front
- Effects of Carbonation on Supply of Reactant to Reaction Sites
- Carbonation-Induced Changes in Material Properties

B.2 Diffusion-Controlled $^{14}CO_3^{2-}$/Grout Tests

- Radiocarbon Uptake Kinetics
- Radiocarbon Uptake Capacity
- Effect of Matrix Properties on Radiocarbon Uptake

B.3 Advection-Controlled CO_2/Grout Tests

- Nature and Extent of Carbonation
- Rate of Advance of Carbonation Front
- Changes in Permeability During Carbonation
- Effect of Carbonation on Supply of Reactant (CO_2) to Reaction Sites

B.4 Advection-Controlled CO_2/Grout/Water Tests

- Nature and Extent of Carbonation
- Carbonation-Induced Changes in Physical and Chemical Properties of Grout
- Rate of Advance of Carbonation Front

Results and Discussion: The key factors affecting grout carbonation have been identified (Table 2), based on existing literature data and our own results obtained to date in this project.

Table 2. Factors Affecting Grout Carbonation

A. Reaction-Controlled Carbonation

- Availability of CO_2 Supply to Reaction Sites
- Grout Composition and Availability of Reactants such as $Ca(OH)_2$, etc.

B. Reaction & Transport-Controlled Carbonation

B.1 Grout Material Properties

- Grout Composition
- Availability of Reaction Sites
- Material Transport Properties
- Degree of Hydration
- Grain Boundary Effects
- Fractures and Microcracks

B.2 CO_2 Flux at the Reaction Front

- CO_2 Concentration
- CO_2 Diffusion/Advection Rate

B.3 Carbonation Effects on Supply of Reactants

- Formation of Interstitial Carbonate Minerals
- Increase in Tortuosity and Reduction in Primary Porosity
- Development of Secondary Porosity
- Production of Water
- Clogging of Pores

The total carbonation capacities determined for the various grout mixes are given in Table 3. These determinations were performed on pulverized grout samples to induce reaction-controlled carbonation, thereby minimizing the constraints the matrix transport parameters are likely to exert in achieving the maximum carbonation. The observed variability in carbonation capacities is a direct function of the varying composition of the grout materials studied. Since the dominant reactive phase in cement providing reaction sites for the carbonation reaction is

$Ca(OH)_2$, the cement content determines, to a large extent, the total carbonation capacity of grout. In fact, the observed values approach the theoretical values, calculated based on $Ca(OH)_2$ content of each grout mix.

Table 3. Carbonation Capacities for the Various Grout Test Materials

Grout Mix	Carbonation Capacity(wt%)
13711	19.25
13712	15.65
13714	19.07
13715	18.90
13716	16.20
13900[1]	19.20
13901[2]	18.70

[1]Mix formulation similar to 13711, but without admixtures. Prepared in March, 1989 for repeat tests.

[2]Mix formulation identical to mix 13900, except Ottawa sand C109 was used in place of natural sand.

Carbonation tests (100% CO_2) conducted at two initial CO_2 pressures exhibit varying degrees of carbonation during the initial stage, indicating that the rate of carbonation is a function of the availability of CO_2 to the reaction sites (7). Solid grout specimens were subjected to elevated CO_2 pressures to investigate the effect of matrix transport parameters on the nature and extent of carbonation. The CO_2 uptake vs time relationship for a solid grout sample is depicted in Figure 1. Relative to the maximum carbonation capacity determined for the pulverized grout sample (Table 3), Figure 1 indicates that the carbonation levels achieved for solid grout samples are considerably lower, approaching 9-10%. As indicated in Figure 1, further CO_2 uptake was observed (5-6%) upon recarbonation after the initially carbonated sample was allowed to dry for an extended time period. This is further illustrated in Figure 2, showing the effect of successive drying cycles on the recarbonation process. The results presented above clearly demonstrate the limiting effect the build-up of interstitial water, generated as a result of carbonation, has on the supply of CO_2 to the reaction sites, thereby impeding the carbonation process.

Detailed investigations of the reactions of CO_2 with cementitious grout under partially saturated conditions demonstrate the importance of water content on the carbonation process (Figure 3). First of all, virtually no carbonation occurs for samples that have been thoroughly dried, since no free water is present to catalyze the reaction. Secondly, the build-up of water, released during the carbonation process, tends to saturate and block the interconnected pore network, thus preventing access of CO_2 gas to the reaction sites and virtually stopping the carbonation process.

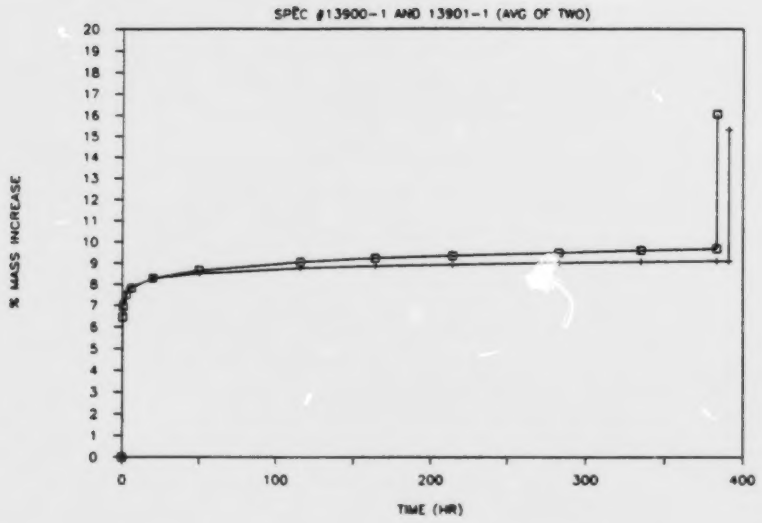

FIGURE 1. % CO_2 uptake versus time for a sample of solid grout. The effect of extended drying (~380 hours) on further CO_2 uptake by specimen is evident.

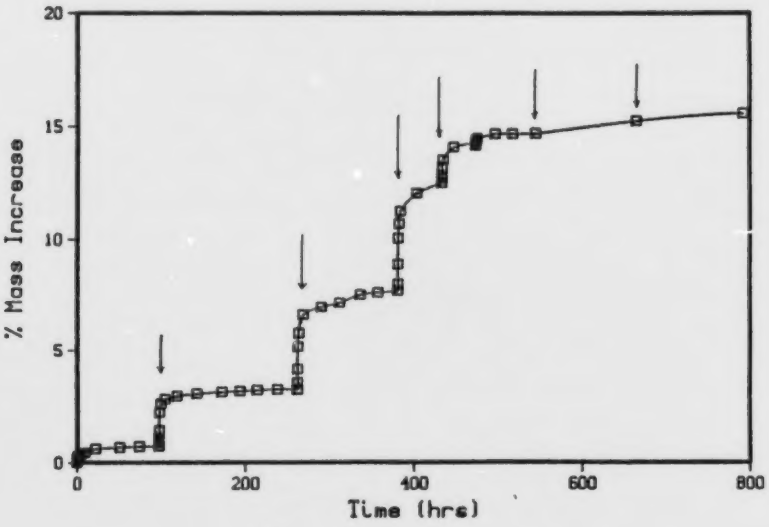

FIGURE 2. % CO_2 uptake versus time for a sample of solid grout. Vertical arrows indicate times at which the sample cell was dismantled and the sample dried under vacuum for several hours (8).

Carbonation of intact grout specimens with 100% CO_2 under water unsaturated conditions is basically diffusion-controlled, as indicated by a linear relationship between CO_2 uptake and square root of time (Figure 4). The observed discontinuities in Figure 4 indicate that the carbonation reaction occurs in three stages, with the completion of the first two stages being relatively rapid. However, it is the third carbonation stage which is of interest with respect to long-term isolation of C-14. This stage reflects a very sluggish carbonation reaction, attributable to the increasingly constricted pore network due to the deposition of carbonation reaction products and free water within the pores. During this stage, both the flux of CO_2 and its availability at the reaction sites are limited by diffusion of the gas through a water saturated pore network and then into the solid grout matrix.

With respect to the overall carbonation of grout over a long time period, it appears that the third carbonation stage has a small effect, relative to the first two stages, on the total amount of carbonation observed for the test material. The limiting effect of the matrix transport parameters on the carbonation process in an intact specimen can be appreciated further when one compares the observations in Figure 4 to the rapid uptake kinetics and extent of carbonation observed for a pulverized specimen (Figure 5).

Further laboratory experiments were performed to study powdered grout/CO_2 interactions in aqueous medium as the degree of carbonation was increased. Particular attention was paid to the nature and extent of grout carbonation, as well as to the evolving mineral assemblage and water chemistry.

This work is important in that it sheds light on the mechanics of grout carbonation which, in turn, is of importance to C-14 attenuation and immobilization in cement-based backfill materials. In addition, prediction of stable end-products and establishment of resultant water chemistry provides further information on the long-term durability and stability of test materials.

The grout material used in the University of Waterloo grout/water reaction experiments was formulated and prepared in the Civil Research Department at Ontario Hydro. The pulverized grout/water solutions were prepared using two different water/solid ratios; namely, 30 g and 15 g of solid in 240 g of distilled water and subsequently equilibrated with three water-saturated gas mixtures: 1%, 5% and 100% CO_2 (balance N_2).

The experimental results for the two solid/water experimental systems at varying levels of CO_2 concentrations are presented in a separate report (9). The results indicate that the carbonation reactions are characterized by the incongruent dissolution of grout mineral phases and precipitation of the reaction products, calcium carbonate and amorphous silica. Under open-system conditions with respect to atmospheric CO_2, the carbonation reactions progress continuously until all available Ca-bearing grout phases have reacted.

The geochemical program, PHREEQE, was used to model the geochemical reactions controlling grout/water/CO_2 interactions and to predict the mineral phases that are likely to exert control on the resultant water chemistry. The simulations further attempt to explain the extent of carbonation observed in the experimental runs.

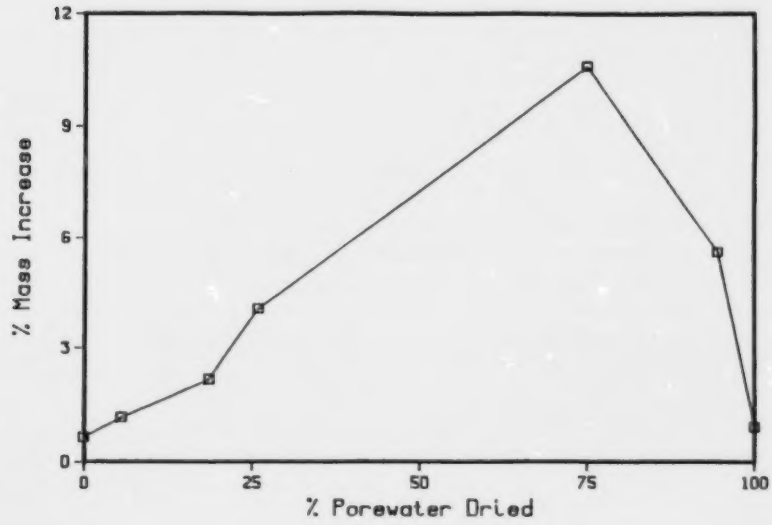

FIGURE 3. The effect of drying on the rate of carbonation. % CO_2 uptake after 1000 minutes of reaction is plotted versus percent porewater dried for a number of samples (8).

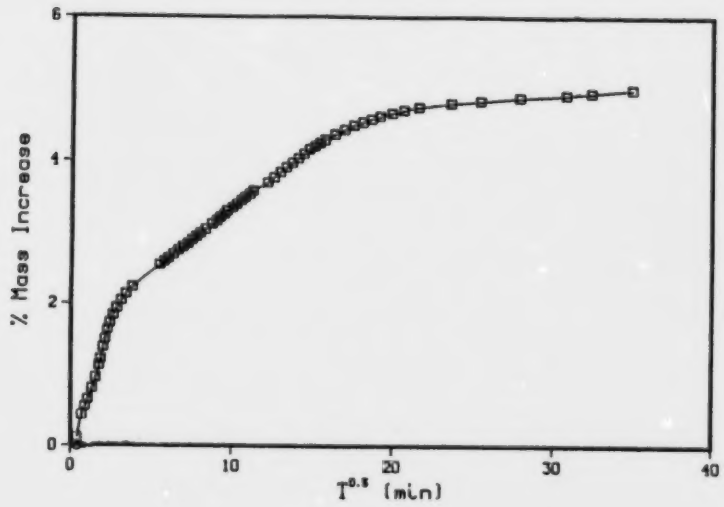

FIGURE 4. % CO_2 uptake versus time for a sample vacuum dried for two weeks and subjected to a p_{CO_2} of 400 psi (8).

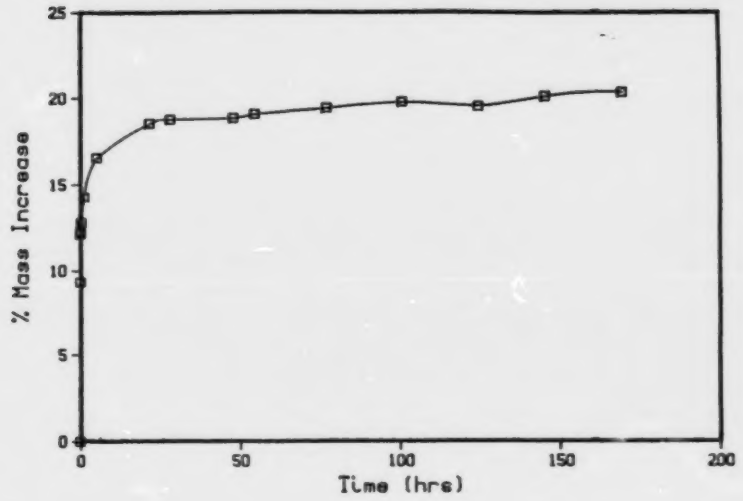

FIGURE 5. % CO_2 uptake for a sample of powdered grout (8).

Based on the simulation runs, three main stages of the carbonation sequence can be delineated:

- an initial stage, marked by small changes in pH and pCO_2 during grout dissolution
- an intermediate stage, marked by sharp changes in pH and pCO_2
- a final stage, characterized by an approach to constant pH and pCO_2

Comparison of the pH data from the simulation and experimental runs helps to explain the sequence and extent of carbonation observed in the experimental runs. For example, in:

- 1% CO_2 system: solid materials are carbonated to completion (dominated by carbonation of the solid phases)

- 5% CO_2 system: dominated by carbonation of the solution phase, following carbonation of the solid phase (drastic changes in pH)

- 100% of CO_2: full carbonation of the entire grout/water system approaching equilibrium, as reflected by constant pH values

The predicted changes in the mineral assemblage during the three stages of the simulation of grout/CO_2/water reactions are depicted in Figure 6 and summarized as follows:

Carbonation sequence

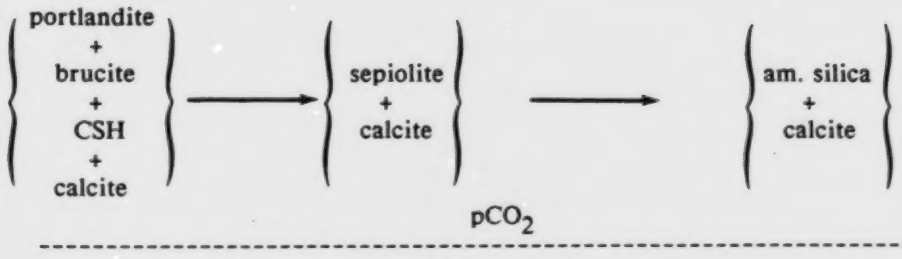

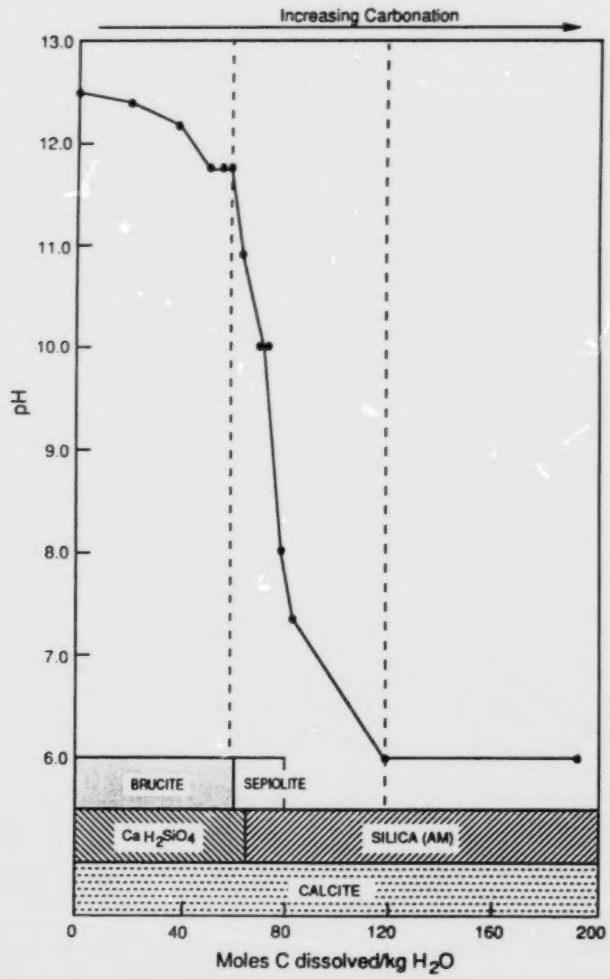

FIGURE 6. Simulation of progressive carbonation reaction in a grout/water system, showing the predominant mineral phases exerting control on the evolving solution chemistry (7).

As evident from Figure 6, the starting point for the grout/water carbonation reaction simulation is portlandite equilibrium. Upon addition of carbonic acid (CO_2(aq)), however, this equilibrium is quickly disturbed, with brucite, calcium silicate, and calcite exerting control on the evolving water chemistry. Since both Ca^{2+} and CO_3^{2-} are predominant in the aqueous system, calcite stability is maintained throughout the simulation and will be omnipresent during the entire grout carbonation reaction.

The dashed vertical line in Figure 6 delineates the end of the initial phase of carbonation, indicating that the grout has been fully reacted. The intermediate phase is characterized by carbonation of the solution phase, as depicted by drastic changes in pH. During this carbonation phase, the solution initially exhibits equilibrium with respect to sepiolite and amorphous silica. However, with increasing degree of carbonation, the pH drops below 10 at which sepiolite is unstable. The final phase, reflecting complete carbonation, is characterized by the presence of the stable end-products, amorphous silica and calcite, which exert control on the final solution chemistry.

In summary, the above simulation based on PHREEQE provides insights into the nature and extent of carbonation taking place in the experimental runs. For example, in the 1% CO_2 runs, the carbonation reaction progressed to the point at which the solid material was fully carbonated and, upon further addition of CO_2 (such as that in the 5% run), it is the solution phase that is being progressively carbonated as reflected in drastic decreases in pH. On the other hand, in the 100% CO_2 runs, sufficient carbon was added to the aqueous system to result in rapid carbonation of both the solid and solution phases, corresponding to an accelerated carbonation process.

More recent work at the University of Waterloo (12) has provided data for development of a model to simulate progressive chemical changes that accompany the carbonation of a grout/water system. The results indicate that the equilibrium model provides a good representation of the experimental data and can be used to delimit carbonation-induced reaction paths in a grout/water system, revealing the progressive changes in solution chemistry and mineral masses, as well as the appearance or disappearance of mineral phases with time.

Reactant flow-through carbonation experiments were carried out to determine the nature and degree of carbonation under advective carbonating conditions. The flow-through test configuration for grout carbonation provides more conducive conditions for the carbonation reaction in that the reactant can be transported through the porous matrix directly to the reaction sites. Compared to diffusion-controlled carbonation, advective transport is a more effective method for carbonating solid grout samples due to the increased availability and supply of CO_2 to the reaction sites. Another advantage of the flow-through setup is that information on progressive changes in material permeability, induced as a result of increasing carbonation, can be obtained.

Most laboratory tests conducted at Ontario Hydro have involved studies of CO_2/grout interactions under advective carbonating conditions. An attractive feature of the test method is its versatility in allowing both nitrogen and carbon dioxide to be used sequentially in a repetitive mode, so that the effects of induced carbonation on material permeability could be evaluated. Further details of the test methodology used at Ontario Hydro for studying solid grout carbonation and the resultant changes in permeability are discussed elsewhere (10).

Based on the results obtained to-date, the grout materials exhibit a high reactivity for CO_2 yielding carbonation products which have the potential to immobilize radiocarbon. Repeat tests using nitrogen gas demonstrate that the test materials, when subjected to successive carbonations, exhibit a progressive decrease in permeability with increasing degree of carbonation (Figure 7). Some of the important carbonation-induced changes in material properties include, with increasing degree of carbonation, a progressive reduction in porosity, permeability, pore size, and an increase in the specific surface area. The changes induced in the material transport properties for grout mix 13711, as a result of carbonation, are summarized in Table 4. More recent gas permeability tests (pressure decay and constant pressure) performed on test specimens, before and after induced carbonation, reveal a significant reduction in gas permeability following carbonation (Figures 8 and 9). Recent data obtained by the Waterloo group also indicate a decrease in the flow rate of the influent CO_2-spiked solution over time due to carbonation-induced reduction in sample porosity. Thus, the carbonation resulted in a significant decrease in permeability (12).

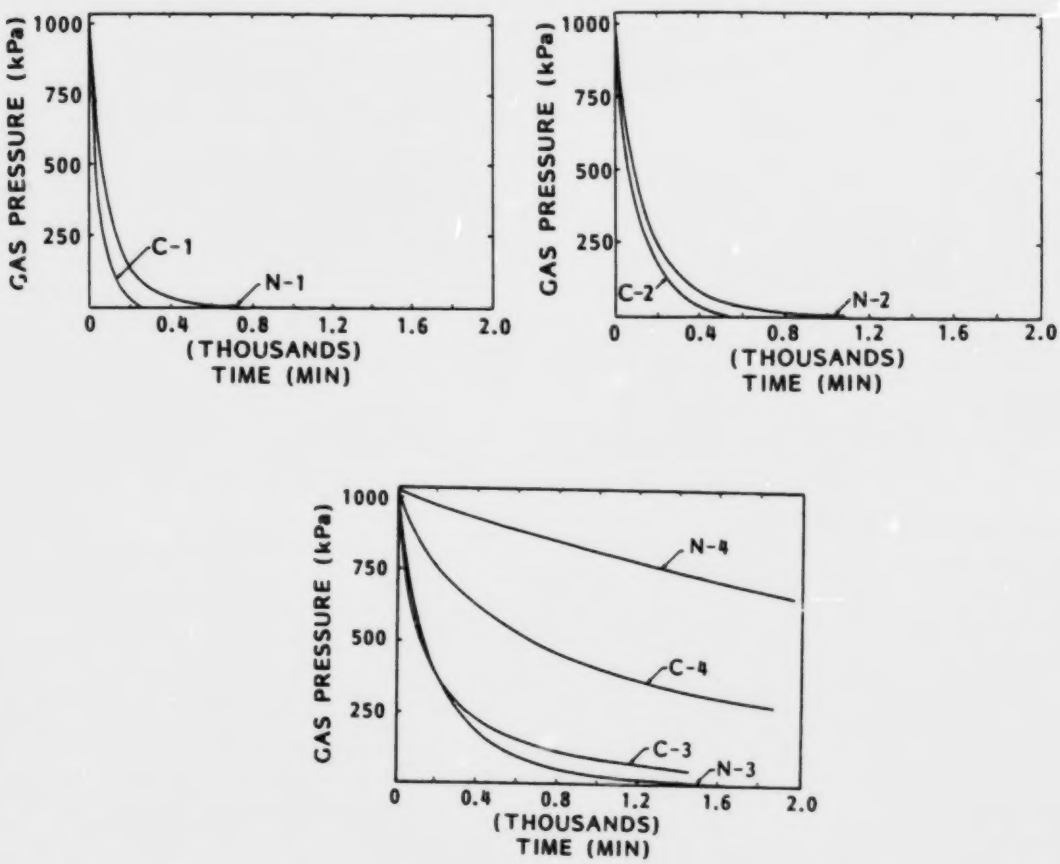

FIGURE 7. Nitrogen and carbon dioxide pressure decay tests show the effect of successive carbonations (C-1, C-2, C-3, C-4) on material permeability (N-1, N-2, N-3, N-4).

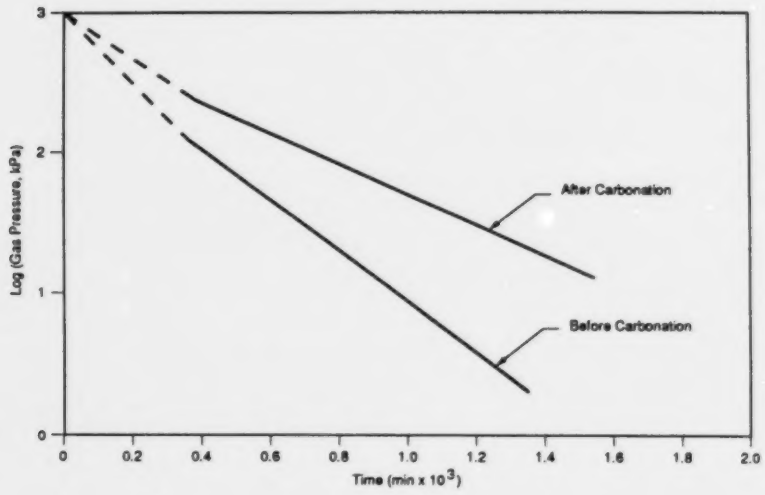

FIGURE 8. Nitrogen pressure decay curves for test specimen 13901 before and after carbonation, showing an exponential relationship and a decrease in permeability following carbonation.

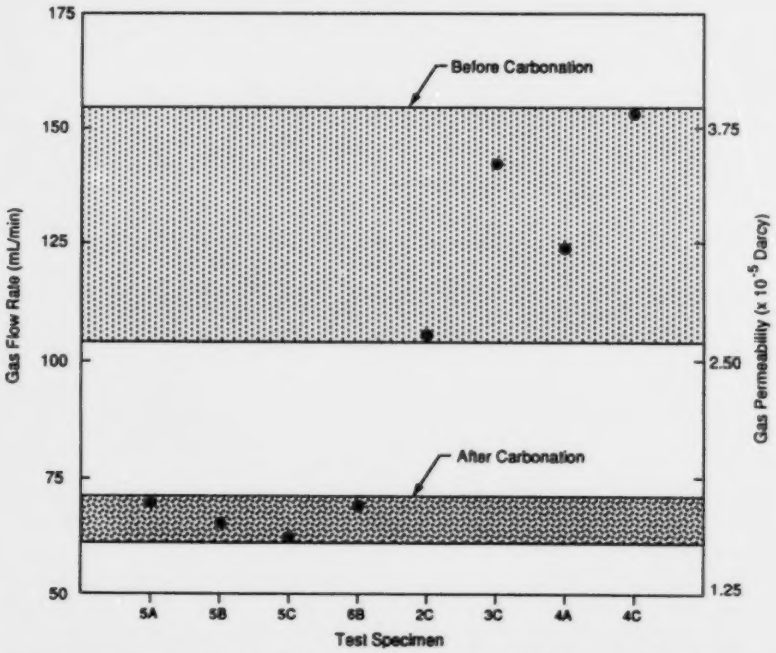

FIGURE 9. Constant pressure flow tests on Specimen 13901, indicating a reduction in permeability following carbonation. The vertical extent of the shaded areas reflects the range of gas flow rates and corresponding permeabilities based on four determinations on replicate samples.

Table 4. Changes Induced in Material Transport Properties as a Result of Carbonation[a]

Material Property	Before	After
Porosity (%)	22	17
Gas Permeability (μD)	137	40
Tritium Diffusivity (x 10^{-8} cm^2/s)[b]	1.4	0.62
Tortuosity (x 10^{-4})[c]	1.5	0.67

[a]Based on carbonation tests performed on grout mix 13711.
[b]Based on tritium diffusion tests performed on uncarbonated grout and material sampled from the most carbonated region of the test specimen(10).
[c]Determined from the tritium diffusion values. A value of 9.3 x 10^{-5} cm^2/s was used for self-diffusion coefficient of tritium in free solution.

Microscopic examination of the carbonated test material under polarized light reveals a highly carbonated cement paste (Figure 10). A close-up of the same section shows the presence of reaction rims of calcitic material around silicate grains in addition to a highly carbonated cement paste (Figure 11). Further examination reveals the presence of microfractures in the cement paste that are filled with calcitic material (Figure 12). With increasing distance from the carbon source, however, the cement paste exhibits a granular, mottled texture, completely devoid of any carbonation alteration features, i.e., similar to that of the non-carbonated material (Figure 13).

The laboratory results obtained to date in this program have established that carbonate uptake on grout involves a chemical reaction between the CO_2 and $Ca(OH)_2$/CSH* phases in cement, thereby resulting in the irreversible fixation of CO_3^{2-} as calcite in the matrix. It has been further established that the rate and extent of carbonate uptake on grout is determined largely by the availability and flux of the reactant to the reaction sites. In light of these observations, the migration and transport of C-14 in grout backfill cannot be modeled by a simple equilibrium Kd approach. Preliminary results of additional tests performed to evaluate $^{14}CO_3^{2-}$ uptake on grout indicate that the final extent of the uptake reaction is dependent on the initial C-14 concentration in solution.

As part of this program, it has been suggested in an earlier report (9) that C-14 would not be leached from the waste site until the carbonation capacity of the grout backfill has been attained through either diffusive or advective transport of dissolved inorganic carbon (DIC) in groundwater. Assuming the initial matrix transport parameters of grout backfill to remain unchanged over long time periods and using a representative groundwater DIC concentration of 3.0 x 10^{-3} moles/litre, it was estimated that the minimum time required for complete carbonation of a meter thick grout backfill barrier would be several times longer than the half-life of C-14, during which time all C-14 will have decayed to background levels. Although an interesting approach, it is too simplistic in its application to the C-14 disposal problem for the following reasons.

* calcium silicate hydrate phase

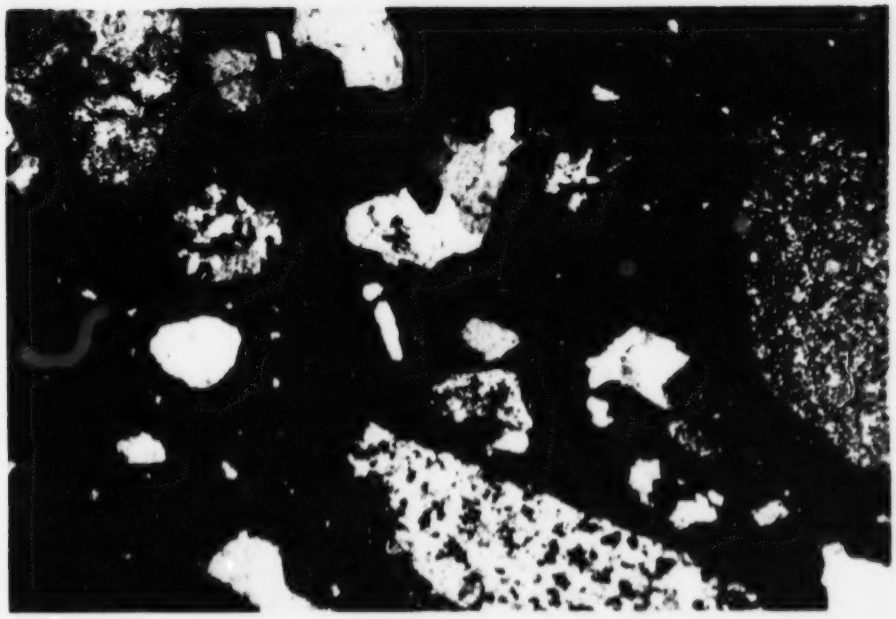

FIGURE 10. Photomicrograph showing a highly carbonated paste (crossed nicols, 10X).

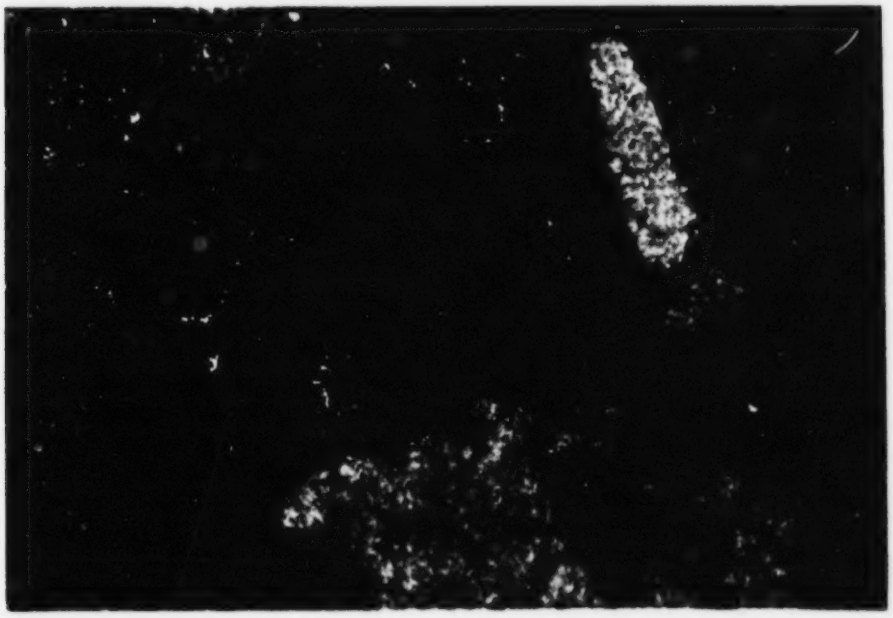

FIGURE 11. A close-up of photomicrograph in Figure 10, showing reaction rims of calcitic material around silicate grains, as well as a highly carbonated cement paste (crossed nicols, 40X).

FIGURE 12. Photomicrograph showing microcracks filled in with highly birefringent calcitic material, as well as reaction rims around silicate grains and a relatively less carbonated cement paste (crossed nicols, 40X).

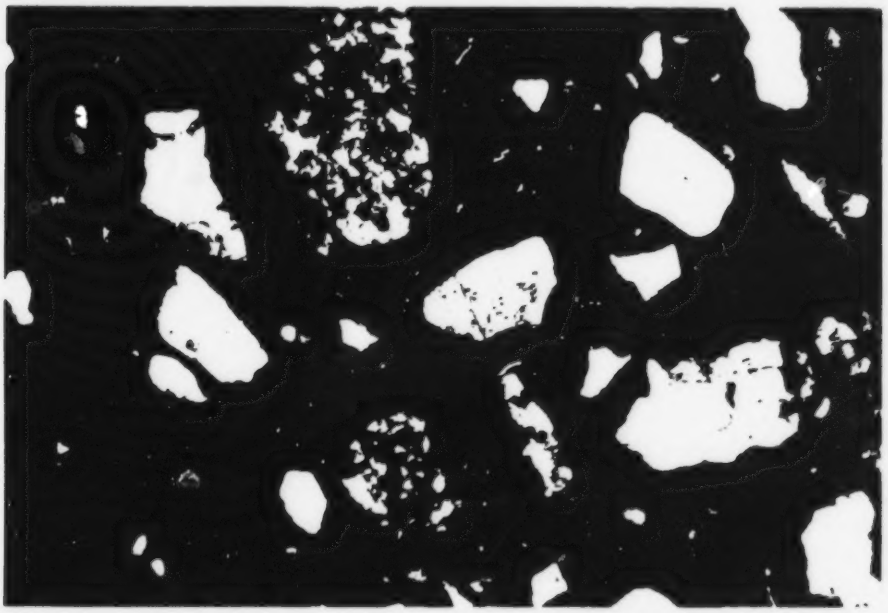

FIGURE 13. Photomicrograph showing cement paste with a granular, mottled texture, completely devoid of any carbonation features (crossed nicols, 10X).

First of all, a cement-based engineered barrier cannot be assumed to maintain its physical and structural integrity for time periods in the order of 10^4 to 10^5 years. In fact, demonstrating even a 500-year life for a concrete high integrity container, based on short-term laboratory data, is problematic. Secondly, our laboratory results have established that maximum carbonation capacities are not attained for intact test specimens. The reason being that, following the initial carbonation, the matrix transport parameters tend to control the availability and flux of the reactant to the reaction sites located beyond the carbonation front in the specimen. Carbonation-induced changes in material transport properties, together with the generation of water occupying the matrix interstices, impede the transport of the reactant to the reaction sites. This results in a significantly lower rate and degree of carbonation (in their calculations (9), the maximum carbonation capacity for grout, measured on a pulverized sample, was used). Since these induced changes, as well as the generation of water in the carbonation reaction, are known to exert a limiting effect on subsequent carbonation of grout, the evolving microstructural changes with time will have to be taken into consideration in future modelling of C-14 transport in cement-based engineered barriers.

2.2 SOURCE TERM EVALUATION FOR C-14

Objective: The main purpose of the study is to establish the source term and the ambient near-field chemistry for C-14. Specifically, data on C-14 concentrations and leach rates under a range of groundwater flow conditions are established, paying particular attention to the geochemical processes controlling the source term characteristics.

Work Plan: The overall work plan includes the following:

- Investigation of the leaching behaviour of ^{14}C-spiked cemented waste
- Evaluation of the effects of groundwater flow rate on C-14 leach rates and near-field chemistry
- Determination of leach rates for C-14 under a range of leachant flow conditions to establish bounds on the source term

Description of Laboratory Work: Cemented waste forms, with a water/cement (w/c) ratio of 0.40 and spiked with 20μCi of C-14, have been leach tested under both static and dynamic flow conditions. The leaching configuration selected allowed single-face leaching of the waste form in deionized water, similar to the test methodology developed by Hespe (13). Under dynamic leaching conditions, the leachant was replenished continuously using a peristaltic pump at two pre-determined flow rates (0.38 mL/min and 0.04 mL/min). Leachate aliquots were collected periodically and analyzed for both the C-14 content and pH. For the two dynamic leaching systems, the flow rates, which were pre-set by appropriate selection of pump speed and tubing size, were monitored with time. Subsequently, a new set of leaching tests, containing no C-14 in the waste form, was started to monitor the release of inactive constituents such as Ca, Mg, Na, K, Si, Al, dissolved inorganic carbon (DIC), and pH from the cement matrix over time. This information is needed to establish the mechanisms by which C-14 is released from the waste form under the range of leaching conditions described above.

Results and Discussion

Preliminary research in this project has established that the leachant flow rate has a pronounced effect both on the near-field chemistry and the leaching behaviour of C-14. At both static and low flow conditions (0.04 mL/min), the near-field chemistry is dominated by a strongly alkaline environment determined primarily by portlandite solubility (Table 5). Under these conditions, no detectable C-14 was observed in the leachates, indicating that the C-14 present in the grout is fixed and not readily leachable.

Table 5. Effect of Flow Rate on C-14 Leach Rates[a]

Flow Rate	pH	Leach Rate (s^{-1})[b]
High flow (0.38 mL/min)	9.0 - 7.5	2.5×10^{-9}
Low flow (0.04 mL/min)	10.5 - 9.5	c
Static	12.5	c

[a]After 160 days of leaching, representing steady-state conditions.
[b]Geometric surface area of grout exposed to leachant is 63.6 cm^2.
[c]C-14 activity levels are below detection.

At the high flow rate, however, the leachant residence time is too short for portlandite to exert a solubility control on the near-field chemistry. Accordingly, the observed pH lies in the range 9.0 - 7.5, reflecting a coupled effect of chemical reaction and physical dilution of the leachate. At these near-field pH and flow conditions, detectable C-14 concentrations are observed in the leachate, yielding a steady-state incremental leach rate of approximately 2.5×10^{-9} s^{-1}, after a leaching period of ~160 days.

Assuming all C-14 to be present in the form of calcite, the observed C-14 release behaviour can be attributed to the dissolution of calcite under the leachant flow conditions studied. Under static leaching conditions, our observations indicate that portlandite exerts control on the near-field chemistry. Since a solution in equilibrium with portlandite is oversaturated with respect to calcite, no dissolution of calcite and hence no C-14 release would be expected to occur under these conditions. Similarly, under the low flow conditions, the alkaline near-field environment can be attributed primarily to the dissolution of portlandite. At high pH's, moderate Ca^{2+} and low CO_3^{2-} concentrations, the rate of calcite dissolution is reported to be extremely low(14).

Calculations were performed to establish calcite solubility curves as a function of pH for two different concentration levels of dissolved inorganic carbon (5 and 100 ppm). The pH-Ca^{2+} relationship is displayed in Figure 14. The data points represent the steady-state calcium

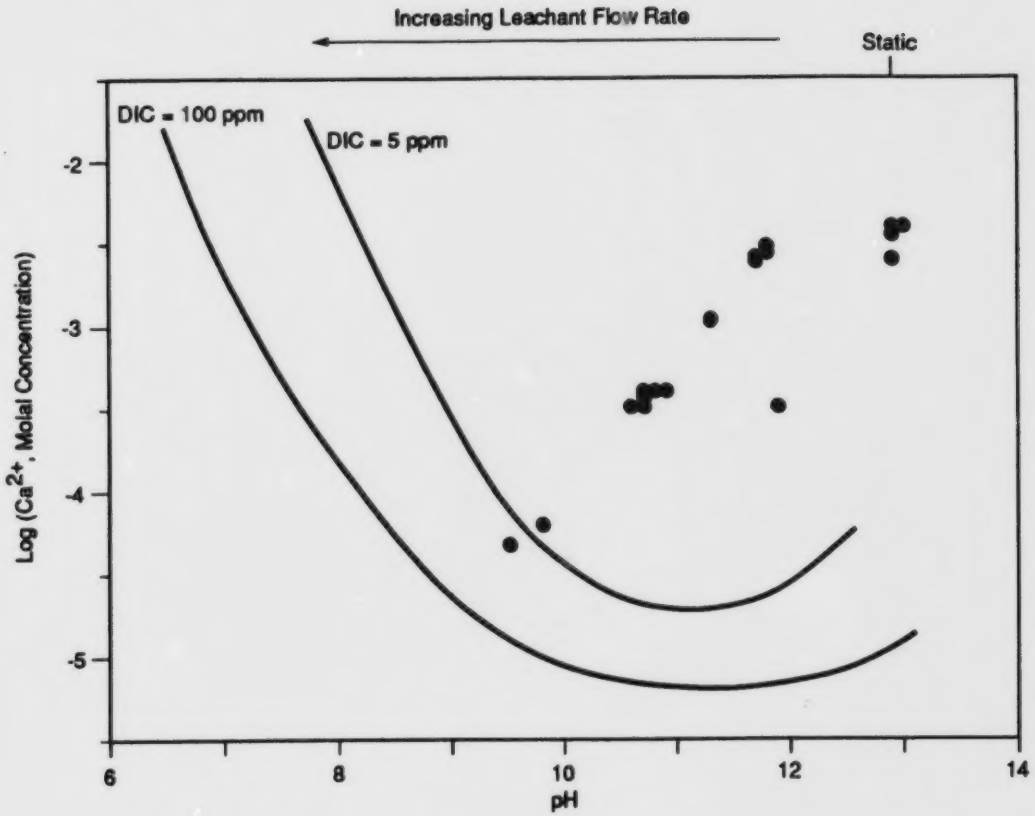

FIGURE 14. Ca^{2+} - pH relationship showing calcite solubility as affected by pH, for two concentration levels of DIC. The data points represent steady-state pH and Ca^{2+} concentrations observed at varying leachant flow rates.

concentrations and pH values observed under static, as well as under both low and high flow dynamic leaching conditions. As evident from Figure 14, both the static and low-flow rate leachates exhibit oversaturation with respect to calcite, indicating that calcite will not undergo dissolution under these leaching conditions. This is consistent with our observations of no C-14 release under static and low flow leaching conditions. In contrast, the pH and Ca^{+} concentrations in the high flow conditions indicate that the leachate is undersaturated relative to calcite solubility and, therefore, calcite dissolution will occur. Again, this is consistent with our laboratory observation of C-14 release under high leachant flow conditions.

Under the high flow conditions, however, a linear relationship of cumulative C-14 release with time is observed during the leaching period 126-217 days, with both pH and leachant flow rate being constant (Figure 15). The linear relationship of C-14 cumulative release with time can be explained by the dissolution of calcite in the waste form as the rate-controlling mechanism for C-14 release.

According to Plummer et al. (15), the dependence of calcite dissolution on solution chemistry can be described by:

$$R = K_1 a_{H^+} + K_2 a_{H_2CO_3^*} + K_3 a_{H_2O} \qquad (1)$$

where R is the net rate of dissolution, K_1, K_2, and K_3 are first order rate constants. Under steady-state leaching conditions (leaching period 126-217 days), the activities a_i of H^+ and $H_2CO_3^*$ can be assumed to be constant. In fact, repeat leach testing of inactive grout specimens under varying flow rates indicate steady-state conditions, with pH, Ca^{2+}, and DIC remaining constant over time. Based on eq.(1), this would correspond to a constant rate of calcite dissolution and, hence, C-14 release.

Our preliminary findings have important implications with respect to the C-14 reactor waste disposal problem in that the near-field chemical environment, brought about by the leaching of grout under stagnant or low flow conditions, would promote the retention of C-14 in the solid phase, thereby contributing to the isolation capacity of the waste form for C-14 for an extended time period.

Atkinson et al (16) have reported that, given the use of cement-based materials in a waste repository and the anticipated low groundwater flow rates, alkaline conditions are likely to prevail in the near-field environment of a waste repository for long periods of time (up to 10^5 years). A qualitative description of the evolution of pH within a cement-based repository is presented in Figure 16 (16). Under these anticipated repository conditions, C-14 will remain essentially immobile and its containment by cement-based engineered barriers (waste form, backfill) in a waste repository can be expected for long time periods.

2.3 CONCRETE MATERIALS FOR HIGH INTEGRITY CONTAINERS

Objective: The purpose of the study is to evaluate the durability of normal density concretes for high integrity containers for the storage/disposal of reactor operating waste. The containers are expected to maintain their integrity for the target 300-year service life under anticipated field conditions.

Work Plan: The overall work plan includes:

- Characterization of candidate materials in terms of their physical, material, and microstructural properties

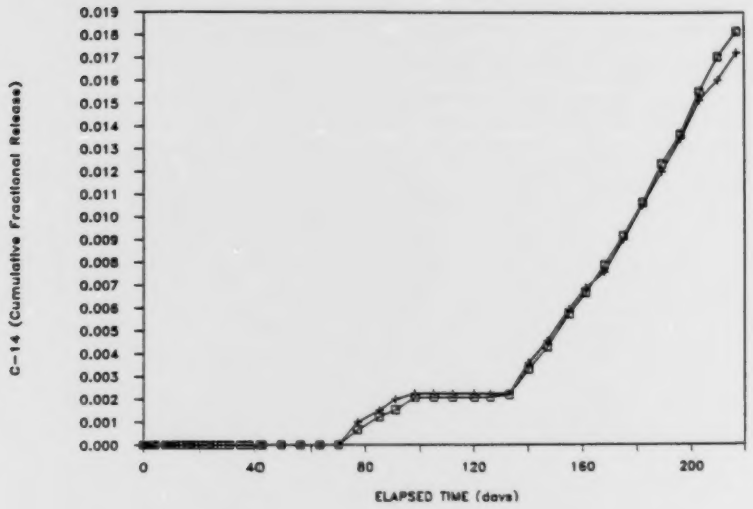

FIGURE 15. Cumulative fractional release (CFR) of C-14 versus time under high flow leaching conditions. (No C-14 was detected in the leachate during the first 70 days due to its absorption by tubing material).

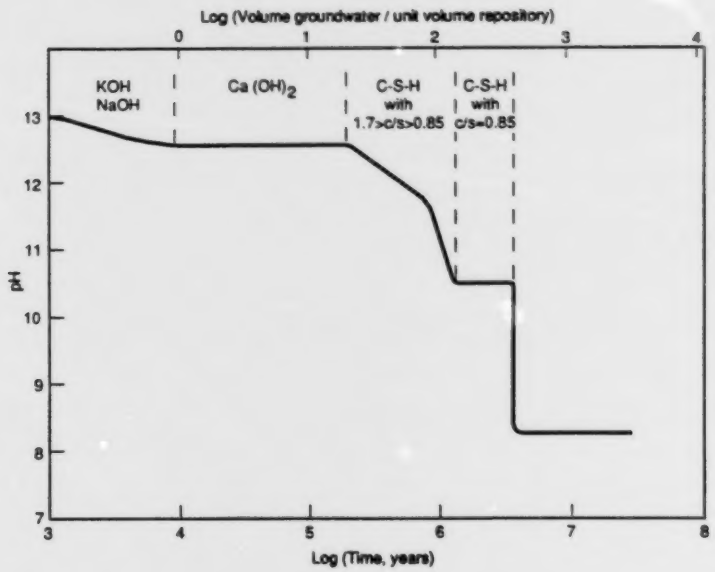

FIGURE 16. The evolution of average pH within a cement-based repository of radius 20 m (16).

- Evaluation of the degree of material degradation and degradation mechanisms due to environmental chemical attack
- Development of a methodology to assess concrete durability
- Development of a generic model for concrete degradation
- Estimation of container life under anticipated field conditions

Description of Laboratory Work: Four mortar mixes were selected for the laboratory testing program, with Sulphate Resistant Portland Cement (SRPC) serving as the control. The other three mixes contain SRPC with varying amounts of Silica Fume (SF) and/or Blast Furnace Slag (BFS) (Table 6).

The chemical compositions of the components, SRPC, silica fume, and blast furnace slag, used in the test mixes, are given in Table 7. Knowing the mix formulations (Table 6) and the compositions of the three components, the final composition of each test mix was calculated (Table 8).

Table 6. Test Mixes and Mix Formulation

Mix	Mix Formulation[a]
13871	100% SRPC
13872	SRPC + 10% silica fume
13873	SRPC + 15% silica fume
13874	SRPC + 30% slag + 10% silica fume

[a]Water/Cement = 0.35; Sand/SRPC + Silica Fume and Blast Furnace Slag = 2.75

Table 7. Chemical Compositions of SF, SRPC and BFS

Component (wt%)	SF	SRPC	BFS
SiO_2	92.70	22.90	37.89
Al_2O_3	0.17	2.80	8.39
Fe_2O_3	0.29	3.64	1.42
CaO	0.17	63.60	38.16
MgO	0.59	3.31	11.55
SO_3	0.36	2.01	2.01
Na_2O	0.16	0.47	0.17
K_2O	0.95	0.45	0.47
TiO_2	<0.01	0.15	b
P_2O_5	0.06	0.06	b
Mn_2O_3	0.02	0.07	0.62
SrO	<0.01	0.04	b
ZnO	0.07	<0.01	b
LOI[a]	3.24	0.68	b
TOTAL	98.78	100.18	100.18

[a]Loss on Ignition, [b]Not Available.

Table 8. Final Compositions of the Test Mixes

Component(wt%)	13871	13872	13873	13874
SiO_2	22.90	29.88	33.77	34.38
Al_2O_3	2.80	2.54	2.41	4.21
Fe_2O_3	3.64	3.30	3.14	2.64
CaO	63.60	57.26	54.08	49.78
MgO	3.31	3.04	2.90	5.51
SO_3	2.01	1.84	1.76	1.85
Na_2O	0.47	0.44	0.42	0.35
K_2O	0.45	0.50	0.53	0.51
TiO_2	0.15	0.14	0.13	0.09
P_2O_5	0.06	0.06	0.06	0.04
Mn_2O_3	0.07	0.06	0.06	0.23
SrO	0.04	0.04	0.03	0.02
ZnO	<0.01	0.01	0.01	0.00
LOI[a]	0.68	0.94	1.06	0.73
TOTAL	100.18	100.18	99.96	100.34

[a]Loss on Ignition.

As a starting point, the laboratory testing program involved evaluation of the physical, material, and microstructural properties, in particular, compressive strength, porosity, pore-size distribution, permeability, and resistance to external chemical attack. The test materials were subjected to static and dynamic leaching/dissolution tests in both deionized water and BNPD groundwater (Table 9) to evaluate their durability in terms of external chemical attack. The two leaching scenarios selected (static versus dynamic) depict different hydrologic regimes and were designed to establish bounds on concrete/groundwater interactions under anticipated field conditions. The major leachate constituents monitored with time included pH, conductivity, Na^+, K^+, Ca^{2+}, Si, Al, and dissolved inorganic carbon. In addition, the microstructural changes induced in the test specimens, as a result of leaching, were determined using polarized light microscopy and gas adsorption porosimetry.

Results and Discussion: Physical testing of the test materials performed in the Concrete Technology Section shows mixes 13872 and 13873 (10% and 15% SF respectively), to have the highest compressive strength (Appendix I). The test mix with blast furnace slag (BFS) exhibited an initially low compressive strength, due to the slow reaction kinectics between portlandite and BFS. As expected, the lowest compressive strength was recorded for the control mix with SRPC (13781).

As seen in Table 10, helium porosity measurements revealed that mortars containing silica fume have lower porosities (by ~13% and 19% for 13873 and 13872, respectively), relative to the control mix. The presence of BFS in mix 13874 results in a slight reduction in porosity (by ~6%) relative to the control mix, but the effect is not as pronounced as that observed with SF. Nitrogen permeability data show a similar trend when SRPC is blended with SF and BFS (Table 10). Similar changes in porosity and permeability for SRPC with additives have been observed in an earlier study (17).

Measurements based on the Rapid Chloride Permeability Technique also indicate a high permeability value for the control mix, whereas the test mortars with SF and BFS exhibit significantly lower permeabilities (Appendix I). Relative to the mortar with 10% SF, both 13873 (15%SF) and 13874 (BFS) exhibit consistently lower permeabilities with curing time.

Table 9. Chemical Composition of BNPD Groundwater

Constituent	Concentration (mg/L)
Calcium	83
Magnesium	38
Strontium	0.2
Sodium	3.5
Potassium	1.8
Aluminum	<1
Dissolved Iron(Total)	<0.05
Magnesium	<0.05
Chloride	24.7
Sulphate	20.9
Nitrate	1.6
Dissolved Inorganic Carbon	36
Dissolved Organic Carbon	1.8
Silicon	3
Hydroxide alkalinity	<5
Bicarbonate alkalinity	292
Carbonate alkalinity	<5
pH (units)	8.3

Table 10. Gas Permeability and Porosity Data on Test Materials

Mix	Permeability (Darcy 10^{-5})	Porosity(%)
13871	2.4	21.8
13872	1.6	17.6
13873	1.9	18.9
13874	2.3	20.0

Using calcium and silica as indicators of matrix degradation, leach data, displayed in Figure 17, clearly illustrates the significantly higher leach resistance of mortars with SF and BFS, relative to the 100% SRPC (mix 13871). As evident from the pH data in Figure 18, the higher leachate pH for SRPC indicates the availability of free $Ca(OH)_2$ for leaching, whereas, in the other

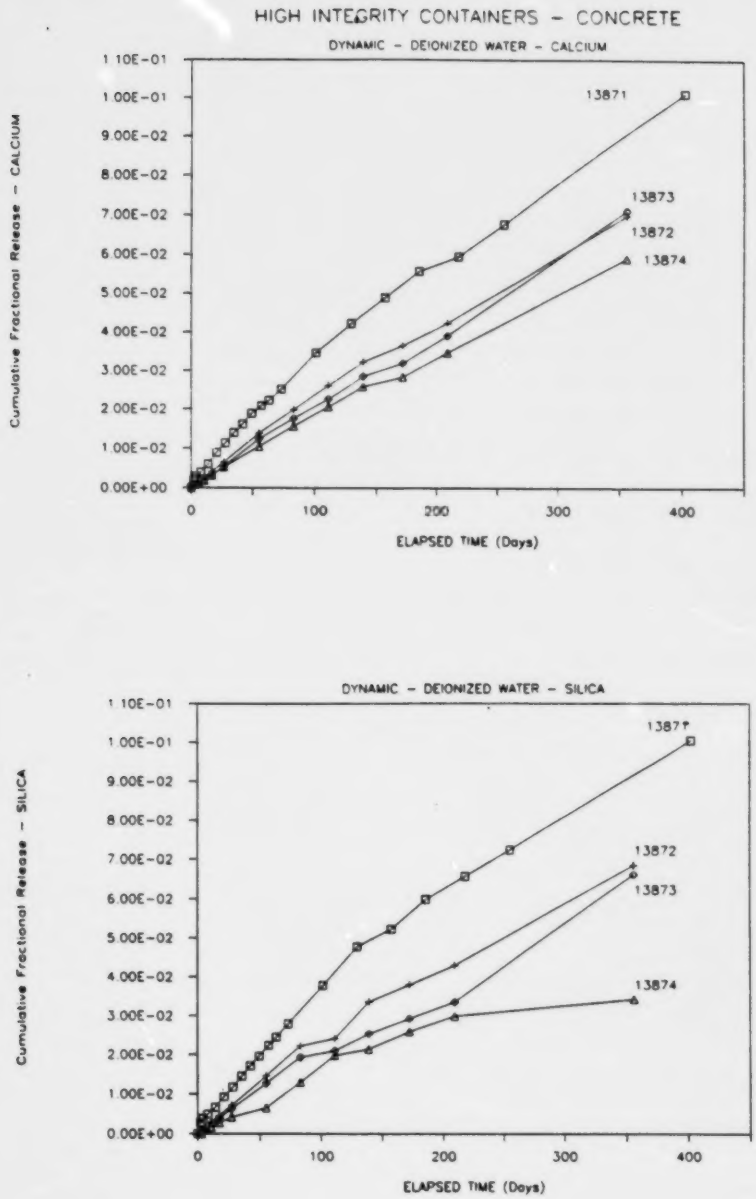

FIGURE 17. Cumulative fractional releases of calcium and silica for the test mixes (13871, 13872, 13873, 13874) subjected to deionized water leaching under dynamic conditions.

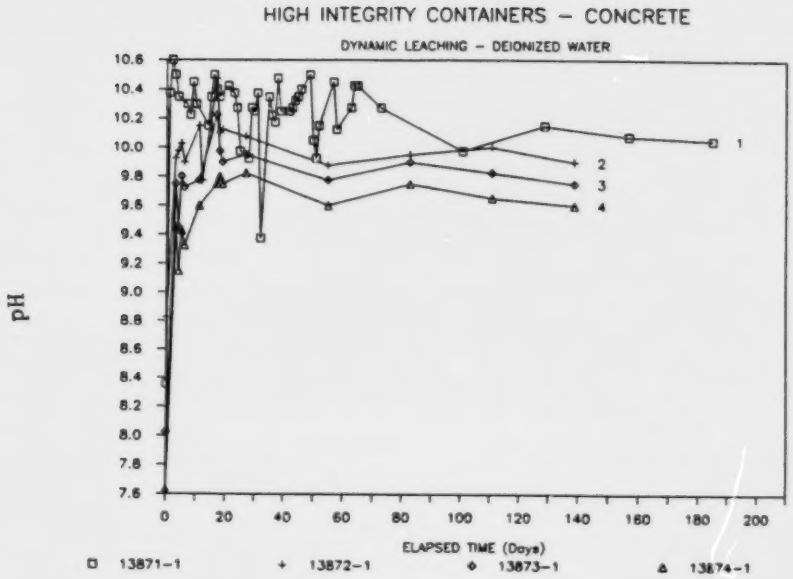

FIGURE 18. Leachate pH versus time for the test mixes (13871, 13872, 13873, 13874) subjected to deionized water leaching under dynamic conditions.

mixes little free $Ca(OH)_2$ is available due to its reaction with SF and BFS to form relatively less soluble calcium silicate hydrate (CSH) and other cementitious phases. This results in lower leachability and, hence, lower leachate pH values.

A close examination of the leach data indicates that mix 13874 (mortar with BFS) is the most resistant to chemical attack, relative to the other test mixes (Figure 17). In general, the mortar with 15% SF exhibits higher leach resistance than that with 10% SF. Overall, the net effect of the additives, with respect to SRPC, is a significant increase in leach resistance, with BFS being the most effective. This is also supported by the leach data for Na and K. The lower reactivity of the test mixes with SF and BFS can be attributed to their lower permeabilities and porosities, as well as a mineralogy composed of relatively insoluble cementitious phases in place of a portion of the free $Ca(OH)_2$ present in the 100% SRPC mix.

Changes in the weight of the test specimens as a result of leaching were recorded (Table 11). As expected, weight losses were observed for all test specimens leached under dynamic leaching conditions. On the other hand, leaching under static conditions resulted in an increase in mass of the test specimens. This is consistent with our leach data. Under dynamic leaching conditions, dissolution and removal of dissolved constituents from the test specimen occurs while under static conditions, precipitation reactions are taking place. This is also supported by microscopic examination of leached specimens, indicating the development of a reaction rim around the periphery of the test specimen during the leaching process (Figure 19). In addition, the presence of reaction rims is also observed around the interconnected vesicles in the leached specimen (Figure 19). The observed reaction rims are most pronounced in specimens leached in BNPD groundwater under static conditions. Under these conditions they approach 0.5 mm in thickness. Microscopic examination of test specimens subjected to dynamic leaching conditions, however, reveal little or no development of a reaction rim.

Further analyses were performed on the leached specimens to evaluate the spatial changes induced in microstructural properties as a result of leaching. Figure 20 shows an increase in surface area and a decrease in the average pore radius for the outer, peripheral radial zone, relative to the interior core of the specimen. In fact, the average pore radius and surface area for the interior core of the leached specimen are very similar to those measured for the unleached specimens (Figure 20). The above observations indicate that the extent of leaching is limited to the outer peripheral zone and that the interior specimen core remains relatively undegraded during the 1-year leaching period. The higher surface areas and lower average pore radii observed for the leached zone may be a result of the deposition of fine-grained, authigenic calcitic material in the pores of the material matrix, as illustrated in the light micrographs in Figure 19.

Using leachate chemistry data, inverse geochemical modeling was performed with PHREEQE to evaluate the geochemical controls on leachate chemistry with time, thus providing important information on the leaching-induced changes as reflected by the evolving mineralogical sequences along the dissolution paths of the concrete-water system.

The following solid phases, which are pertinent to the cementitious system studied here, are considered for the modeling effort: calcite, dolomite, siderite, gibbsite, ferrichydroxide, sepiolite, ettringite, Al-monosulphate, CSH, portlandite, C_3FCsH_{12}, $C_3FCs_3H_{32}$, etc. Only deionized water leachate data was considered at this time for the calculation of saturation indices of potential mineral phases likely to appear or disappear during the dissolution process.

The modeling results indicate that, under static conditions, the leachates for all four mixes exhibit saturation to supersaturation with respect to calcite, dolomite, and sepiolite (Figure 21). The saturation state of the leachates in terms of the CSH phase appears to be affected by mortar composition. For example, leachate 13871 (SRPC, without additives), after being initially undersaturation, exhibits saturation with respect to the CSH phase. In contrast, the other leachates (13872, 13873, 13874) are undersaturated during the entire dissolution period. In contrast, all leachates exhibit undersaturation with respect to both portlandite and ettringite, regardless of mortar composition. However, the degree of undersaturation for mix 13871 is much smaller, relative to the other test mixes. The major reactions involving appearance and disappearance of the key mineral phases controlling the evolving leachate chemistry under static conditions are summarized in Table 12. These reactions represent degradation of concrete under the given conditions described above.

Table 11. Changes in Mass of Test Specimen Following Leaching

Sample No.[a,b]	Mass (g)		
	Initial	Final	Net Change
13871 -1A	c	215.82	c
-1B	c	216.32	c
13872 - 1A	215.36	213.79	-1.57
-1B	219.99	218.66	-1.33
13873 -1A	212.97	210.80	-2.17
-1B	234.25	232.78	-1.47
13874 -1A	222.48	221.12	-1.36
-1B	203.80	202.87	-0.93
13872 -2A	214.56	215.57	+1.01
-2B	221.68	222.55	+0.87
13873 -2A	221.40	222.59	+1.19
-2B	213.63	214.13	+0.50
13874 -2A	217.49	218.77	+1.28
-2B	209.67	210.62	+0.95
13871 -4A	224.37	225.71	+1.34
-4B	210.70	211.93	+1.23
13872 -4A	239.28	240.01	+0.73
-4B	214.43	215.14	+0.71
13873 -4A	208.83	209.44	+0.61
-4B	219.69	222.36	+2.67
13874 -4A	211.04	211.58	+0.54
-4B	214.60	215.15	+0.55

[a]A and B represent duplicate test runs for a given test mix, leachant type, and leaching condition.

[b]Series 1 and 2 represent leaching with deionized water under dynamic and static conditions, respectively. Series 4 represents leaching with BNPD groundwater under static conditions.

[c]Not determined.

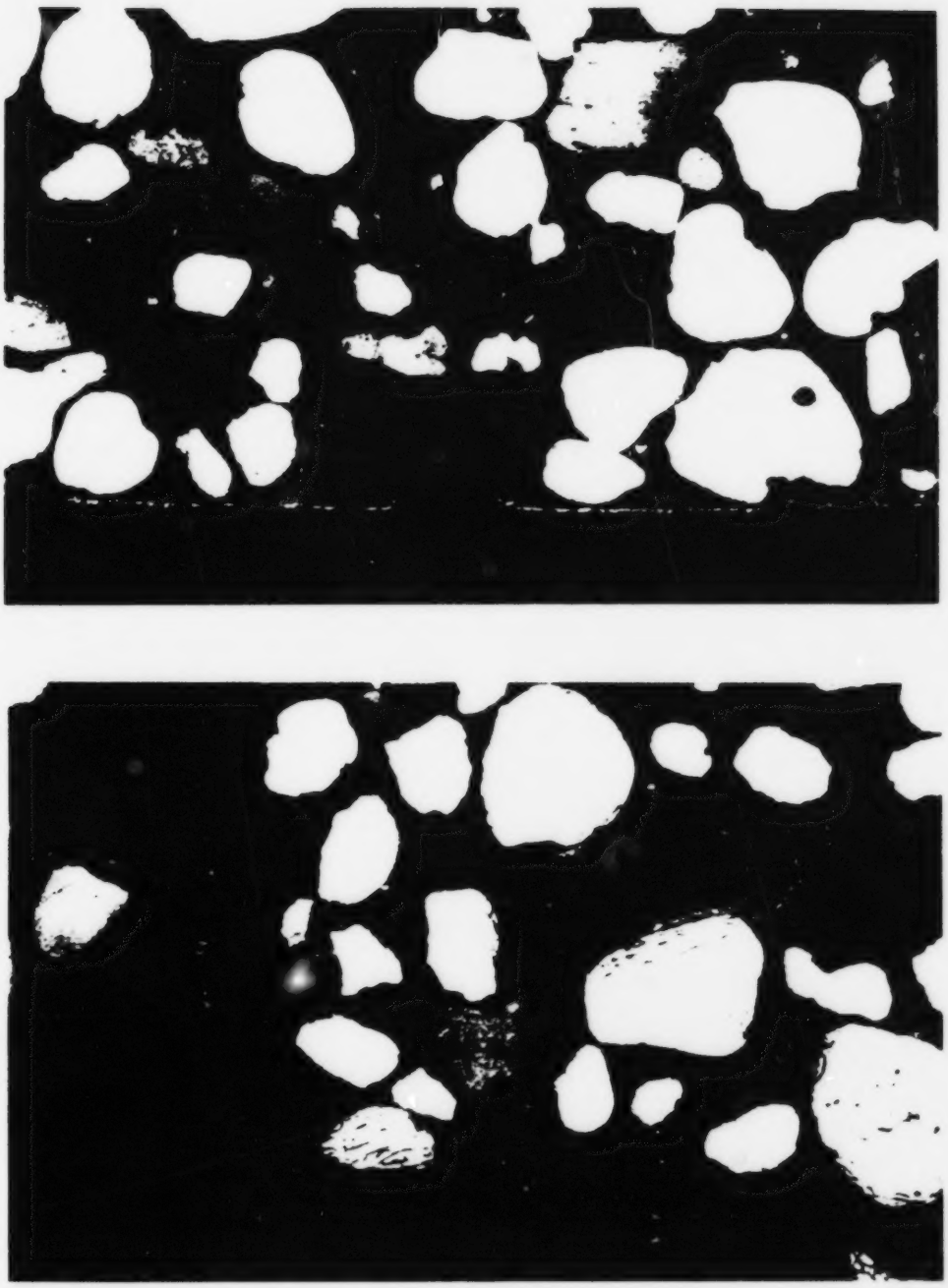

FIGURE 19. Light micrographs of leached specimens showing development of a calcitic reaction rim at the periphery and around the interconnected vesicles in the test specimen.

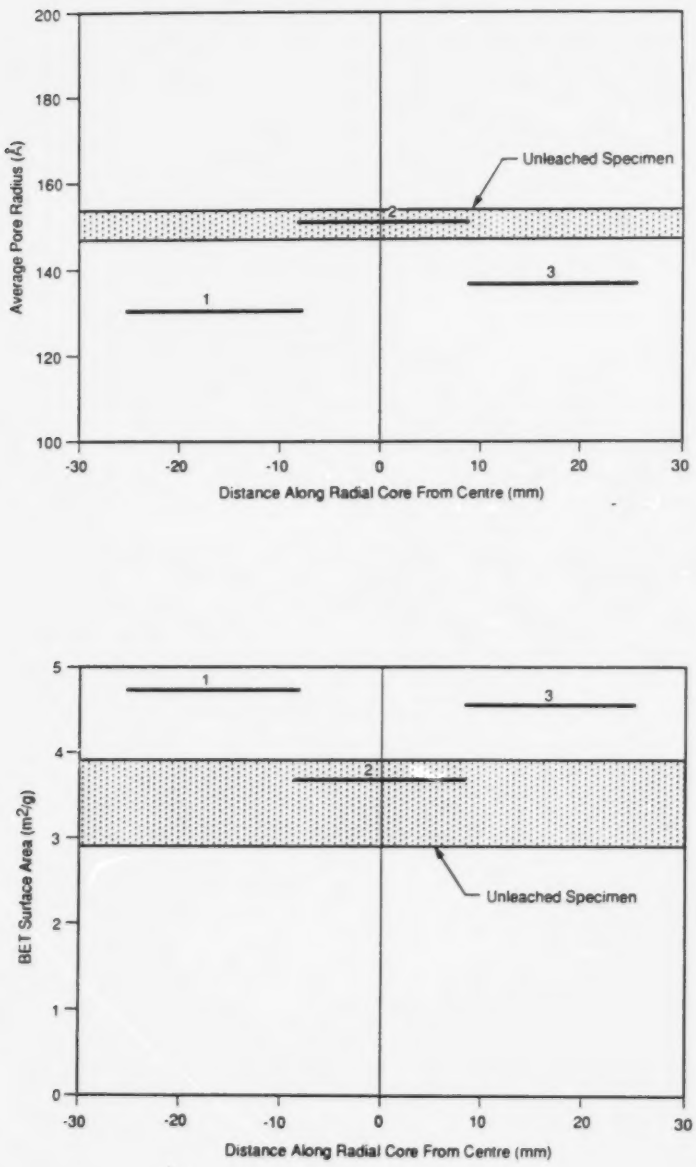

FIGURE 20. Leaching-Induced changes in microstructural properties of the exterior radial zone of test specimen (1,3). The inner core is represented by 2, while the shaded areas represent unleached specimen.

Table 12. Dissolution and Precipitation Reactions Occurring in Concrete/Water Systems

DISSOLUTION	PRECIPITATION
Alkali Metals	Alkali Metals Build-up
$Ca(OH)_2$	Calcite
CSH Phases	Sepiolite
Ettringite	Amorphous Fe, Al Hydroxides

Based on the observed leachate chemistries, our modeling results indicate further that all dissolution reactions discussed above for static conditions are likely to occur for dynamic conditions as well. For the given high flow conditions, our calculations show that the leachates exhibit oversaturation only with respect to calcite. Other mineral phases discussed above are not expected to precipitate out under these conditions. It should be pointed out that, in this particular study, extreme leaching conditions were considered to accelerate the concrete degradation process. In a realistic repository setting, where relatively low groundwater flow rates can be anticipated, precipitation reactions, similar to those discussed under static conditions, are expected to occur.

In summary, under dynamic leaching conditions, the overall leachability for the test mixes (Figure 22) is significantly greater than that observed under static conditions. This is important considering that a waste repository is most likely to be located at a site where groundwater flow is minimal. Considering that test mortars with silica fume and silica fume+blast furnace slag are the most resistant to chemical attack under static deionized water and BNPD groundwater leaching conditions, it can be inferred that these particular concrete materials appear to be the most durable, in terms of external chemical attack, for high integrity containers for storage/disposal of reactor operating waste at the BNPD site.

Further reduction and interpretation of leach data is in progress to assess the nature and extent of material degradation in the context of the IC-57 in-ground container integrity for the target 200-year service life under anticipated field conditions.

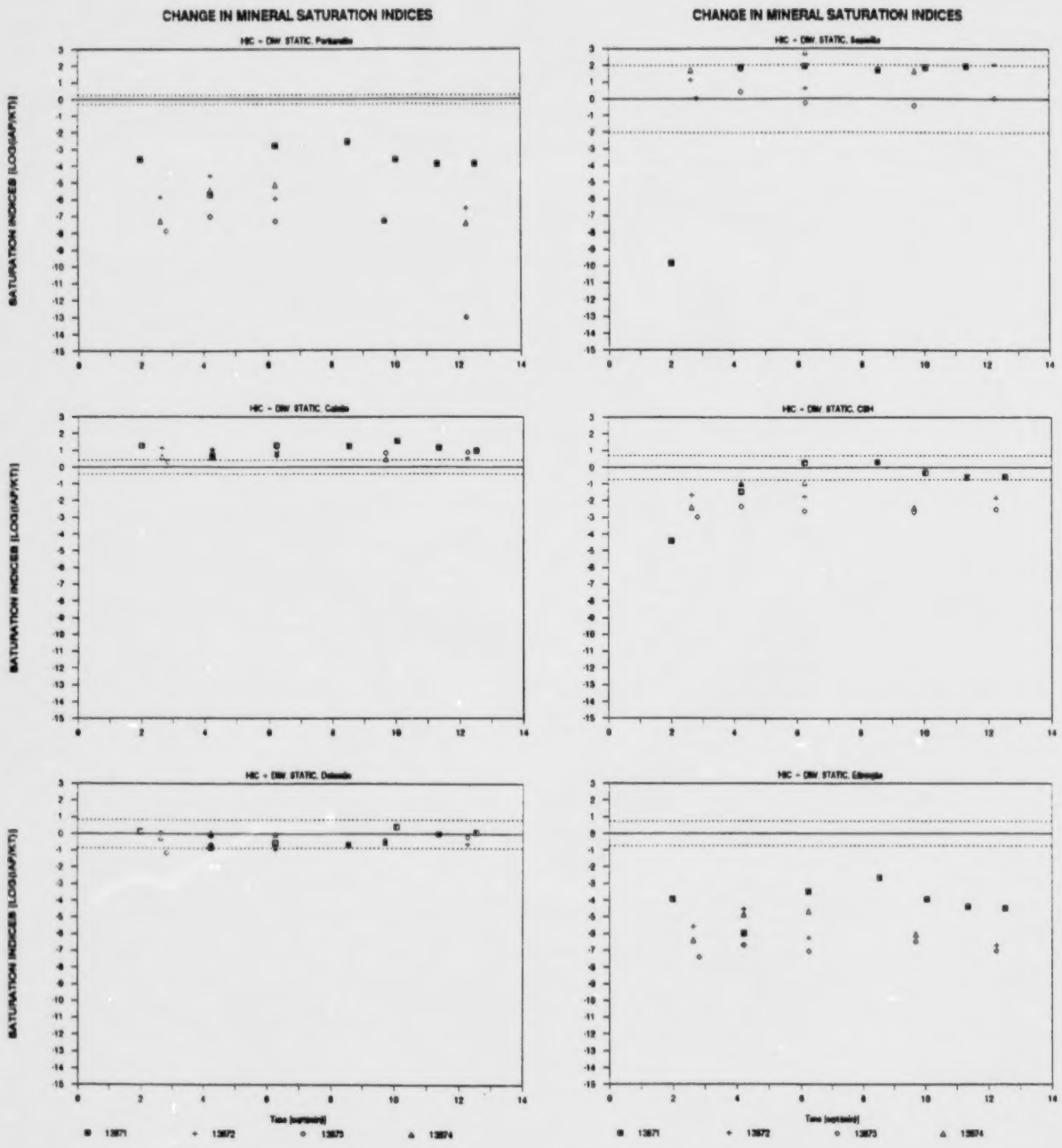

FIGURE 21. Changes in mineral saturation indices with time for the four test mixes subjected to deionized water leaching under static conditions.

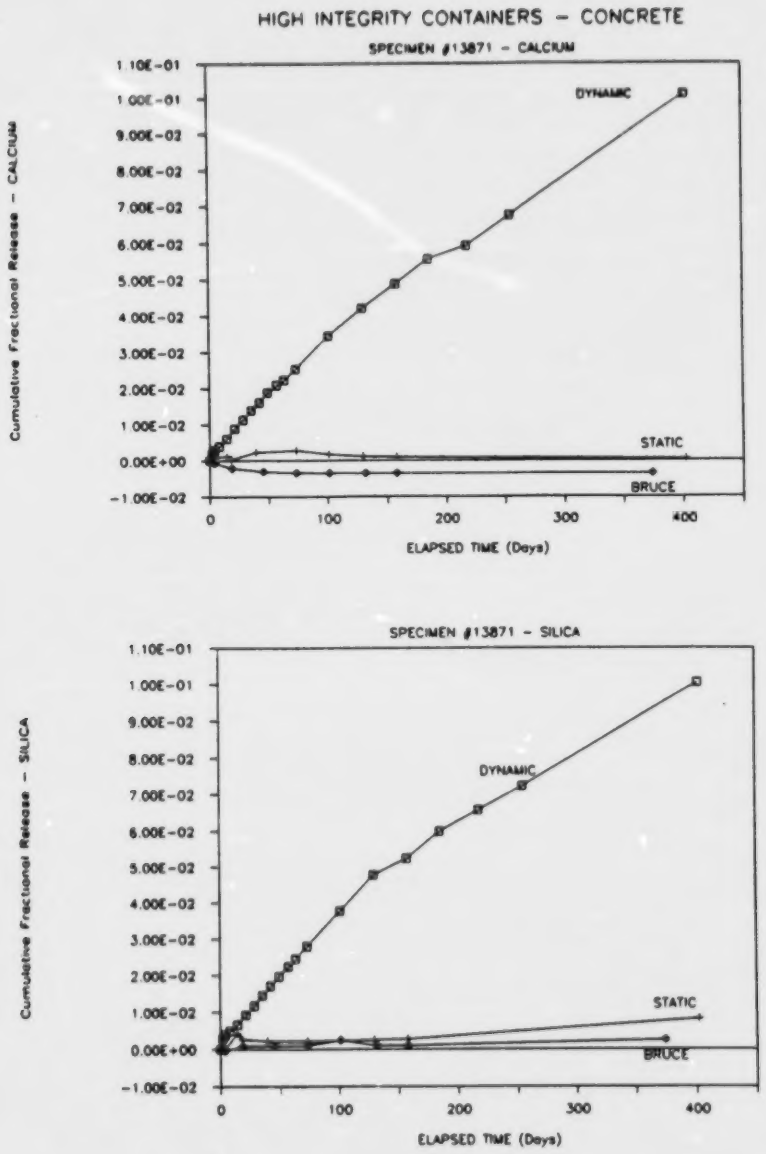

FIGURE 22. Cumulative fractional releases of calcium and silica for test specimen 13871 subjected to both static and dynamic leaching conditions with deionized water and BNPD groundwater as leachants.

2.4 TRANSPORT OF C-14 IN UNSATURATED GEOLOGIC MATERIALS

Objective: The general purpose of this study is to investigate the transport of volatile constituents in partially-saturated geologic materials, specifically, to examine the transport processes for C-14 and to quantify these processes such that they can be represented in mathematical models. Particular attention was given to transport in the gas phase and the associated retardation processes.

In order to model the rate of gaseous C-14 migration in unsaturated porous media, source or sink terms describing the reaction between the liquid and gas, and the liquid and solid phases are required. In view of the significance of gas phase transport and in light of the uncertainties in the magnitude of the liquid-gas exchange rate in partially saturated media, the specific objectives of this research were:

a) to investigate the nature of the reaction term between the solution and gaseous phases

b) to evaluate the relative significance of this reaction on the mass transport of gaseous C-14 in unsaturated porous media.

Work Plan: Laboratory experiments were conducted to examine the rate of transport of gas phase C-14 in an unsaturated porous medium. To reduce the uncertainty in the interpretation of the data, the solid-solution phase transfers were minimized by using a carbonate-free silica sand. The general work plan for the study was to:

- determine the gas-liquid isotopic exchange rates by equilibrium batch experiments under a range of moisture content and pCO_2 conditions
- conduct diffusion experiments for $^{14}CO_2(g)$ to determine the effect of moisture content (air-water interfacial area, cross-sectional area of the gas phase) and CO_2 concentration on C-14 gaseous diffusion coefficients
- incorporate the measured reaction terms into a transport model and evaluate the results against the measured C-14 concentration profiles obtained in the diffusion experiments.

Results and Discussion

The nature of the C-14/C-12 isotopic exchange reaction between aqueous and gaseous phases in partially saturated porous material was studied under a range of moisture content and pCO_2 conditions using the batch exchange system illustrated in Figure 23. The results of the $^{14}CO_2$ uptake experiments are summarized in Figure 24 for the 0.1%, 1% and 10% CO_2 concentrations, respectively. As one would expect, as the water content increases, the C-14 concentration lost to the liquid phase (Co-C) relative to that remaining in the gas phase (C) also rises. Of particular interest, however, is the effect of varying the CO_2 concentration in the gas phase on the C-14 Co-C/C counts ratio. Comparing Figure 24a with Figure 24c for the 7% moisture content, for example, the equilibrium counts ratio increased substantially when the pCO_2 was lowered from 10% to 0.1%. The increase in the concentration of C-14 sorbed with decreasing pCO_2 is most likely due to isotopic fractionation.

The results of the batch experiments also indicate that the kinetics of the exchange reaction is quite fast, with equilibrium being attained within 10-15 minutes for all pCO_2 concentrations studied under all of the moisture content conditions considered. This implies that a kinetic term

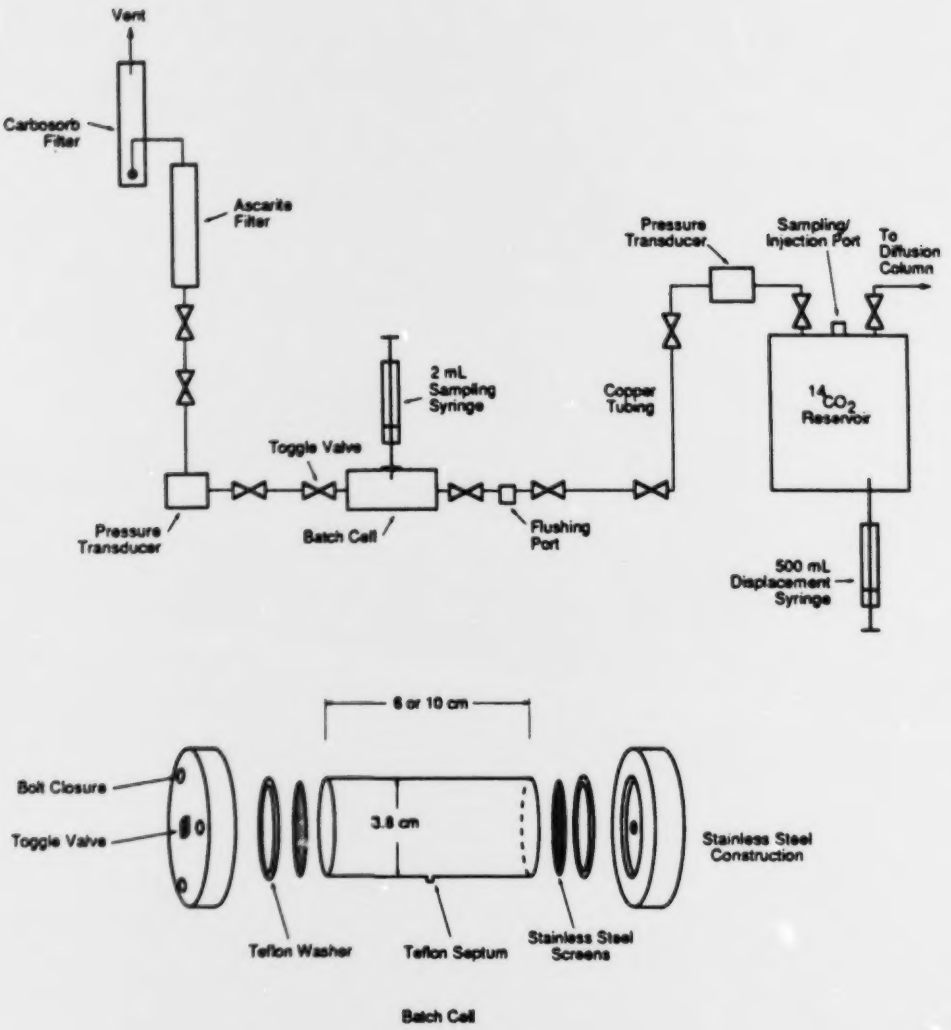

FIGURE 23. Schematic of batch exchange system

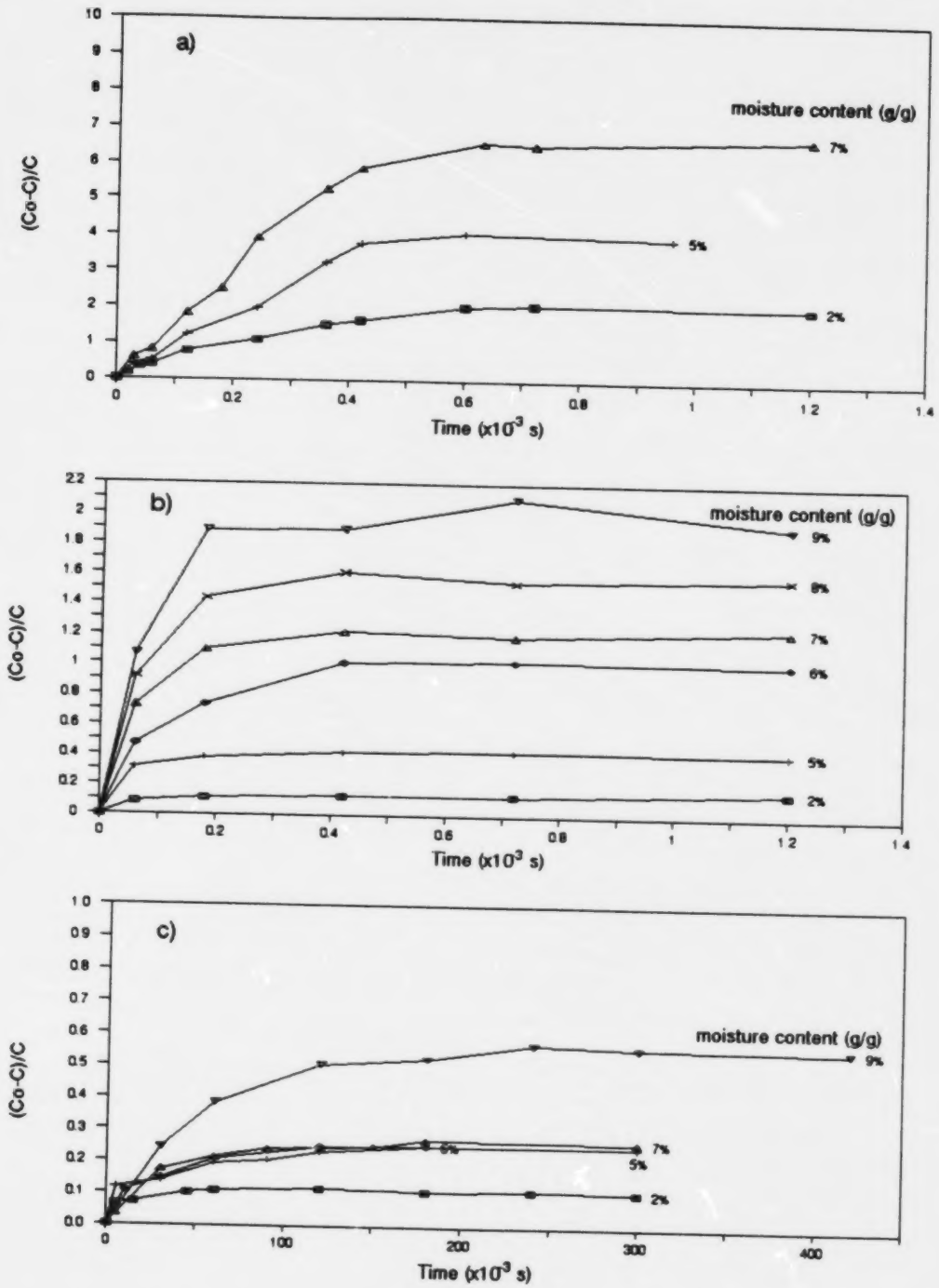

FIGURE 24. C-14 uptake kinetics; (a) 0.1% CO_2; (b) 1% CO_2; (c) 10% CO_2.

may not be required in the mass transport equation and a simpler equilibrium "Kd" approach may be appropriate. Indeed, the results of a desorption experiment conducted at a 5% gravimetric moisture content and pCO_2 of 1% show that the uptake of C-14 from the gas to the solution phase in a partially saturated medium is a reversible reaction, indicating that the use of a distribution coefficient to represent carbon isotope exchange is a reasonable procedure.

Distribution coefficients that characterize the gas/solid (Kd) and gas/liquid (K1) uptake reactions required for input into advection-dispersion equations were calculated and are presented in Table 13.

The calculated gas/liquid distribution coefficients (K1) are of interest since, unlike the relationship between moisture content and the (Co-C)/C counts ratios, we no longer see an incremental rise in K1 with percent moisture. As the moisture content increases, the calculated distribution coefficients, for each pCO_2, tends toward a constant value. The reason for this behaviour is shown in Figure 25. Although the ratio of C-14 lost to that remaining in the gas phase increases linearly with increasing moisture content, this ascending trend is offset by the reduction in the gas-to liquid-volume ratio (V_g/V_l). The result is constant K1 values.

The concept of constant K1 values at variable moisture contents is extremely important since it would enable retardation factors to be calculated for any moisture content from a single measured distribution coefficient. Thus, from the results of the equilibrium batch experiments, under field moisture conditions, it may be reasonable to assume gas/liquid distribution coefficients for C-14 will be constant with respect to moisture, thereby allowing the use of a much simpler transport model for contaminant migration predictions.

Table 13. Calculated Distribution Coefficients

Water Content (g/g)	pCO_2 =	K1 10%	K1 1%	K1 0.1%	Kd* (mL/g)
Dry					0.03
0.02		1.04	1.09	18.6	
0.05		0.75	1.14	12.0	
0.06		0.59	2.11	----	
0.07		0.51	2.28	12.8	
0.08		----	2.06	----	
0.09		0.72	2.42	----	

* all pCO_2 concentrations

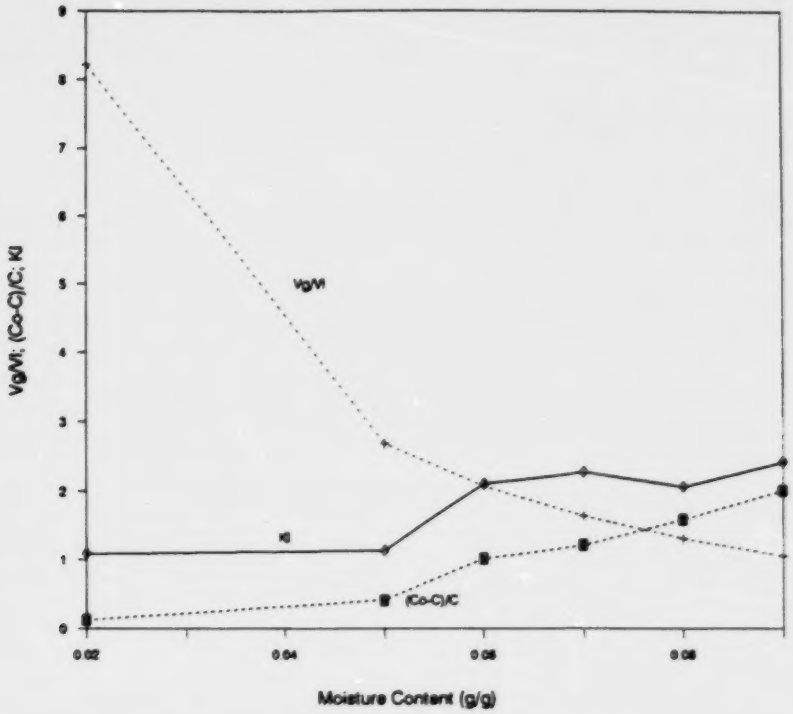

FIGURE 25. Effect of gas-liquid volume ratio on K1 values.

A summary of the measured $^{14}CO_2$ diffusion coefficients are given in Table 14 and an example of the concentration profiles obtained are shown in Figure 26. As seen from Figure 26, the measured profiles were reproducible and showed remarkably little scatter in the C/Co values with respect to the fitted curve (based on Fick's second law) suggesting that the methodology used produces results that are consistent with Fick's second law of diffusion. Measured diffusion coefficients were observed to be extremely sensitive to the gas phase porosity values with sensitivity increasing as the pCO_2 content of the gas phase decreases. For example, as the gas phase porosity is decreased by a factor of 1.5 (from .36 to .24), the measured diffusion coefficient decreased by a factor of 4.5 for the 10% pCO_2 concentration, 13.3 for 1% pCO_2 and 40 for the 0.1% pCO_2 condition. This reduction in diffusion coefficients is a function of both the reduction in accessible pathways due to the increase in porewater plus the effect of isotopic exchange.

The effect of C-14/C-12 isotopic exchange (gas/liquid partitioning) on the diffusive migration of $^{14}CO_2(g)$, in a partially saturated sand is illustrated in Figure 27. The solid line in Figure 27 was calculated from Eq.(2) assuming that adsorption of $^{14}CO_2(g)$ was negligible, thereby giving a retardation factor (R) of 1 (i.e. Kd=K1=0). This equation can therefore be used as a baseline for evaluating the effect of geochemical retardation (specifically isotope exchange) on the diffusive transport of $^{14}CO_2(g)$ in partially saturated porous media.

Table 14. Measured $^{14}CO_2$(g) Diffusion Coefficients

Water Content (g/g)	Gas Porosity	$D_{obs}(cm^2/s)$ pCO_2 = 10%	1%	0.1%
0.0	0.3600	0.0905	0.0872	
	0.3600	0.0895		
	0.3450			0.0789
0.02	0.3260	0.0745		
	0.3260	0.0769		
	0.3102	0.0543		
	0.3050		0.0486	0.0131
0.05	0.2750	0.0381		
	0.2750	0.0331		
	0.2750	0.0361		
	0.2410		0.0200	0.0041
			0.0146	0.0043
0.06	0.2580	0.0363		
	0.2580	0.0339		
	0.2350		0.0137	
0.07	0.2410	0.0226		
	0.2410	0.0199		
	0.2175		0.0064	0.0017
0.08	0.2000		0.0029	
0.09	0.2070	0.0048		
	0.2011	0.0019		

From the above discussion it is therefore anticipated that under conditions more typical of southern Ontario soils (i.e., neutral pH's and carbonate minerals present) the potential effect of isotopic exchange on the diffusive migration of gaseous C-14 will be considerable and should not be ignored in mathematical modeling for pathway analysis.

From Figure 27 it can be seen that, even for a "worse case scenario", that is, for systems containing no carbonate minerals (i.e., liquid/solid exchange is minimal) and under acidic conditions (H_2CO_3 is the dominant carbonate species), isotopic exchange can be significant, particularly as the time frame considered is increased. An example of this is shown in Figure 28 for a gravimetric moisture content of 7% and a time frame of 24 hours. When isotopic exchange is ignored, the contaminant front (gas phase) would have migrated a distance of 136 cm from a continuous source input. If isotopic exchange is incorporated into the model, the migration distances are reduced to 114 cm, 93 cm and 51 cm for the 0.1%, 1% and 10% pCO_2 conditions respectively.

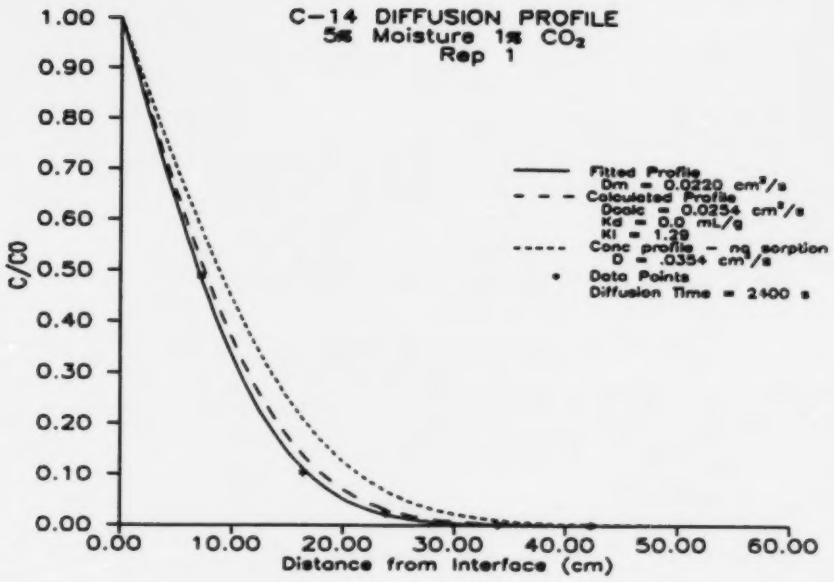

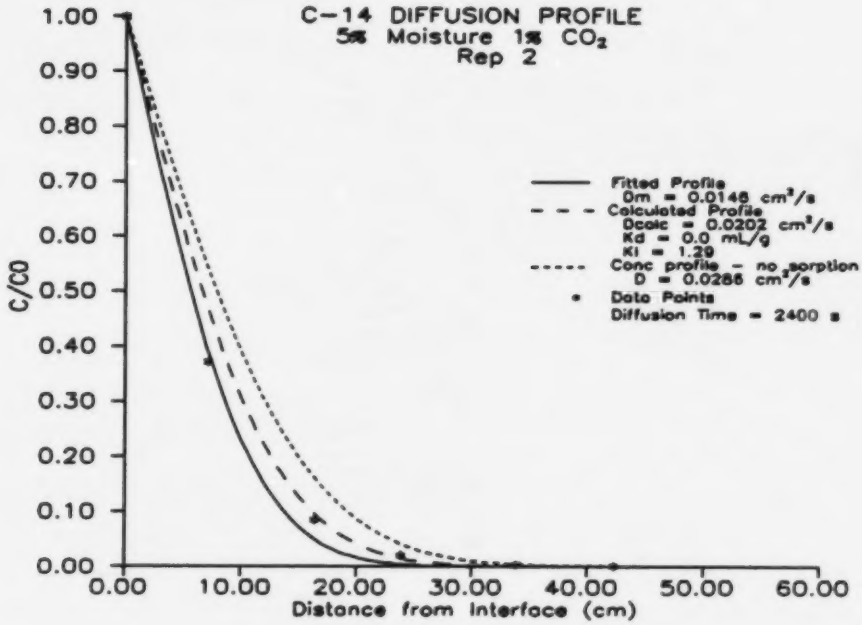

FIGURE 26. Measured $^{14}CO_2$ concentration profiles - 5% gravimetric moisture content, 1% pCO_2.

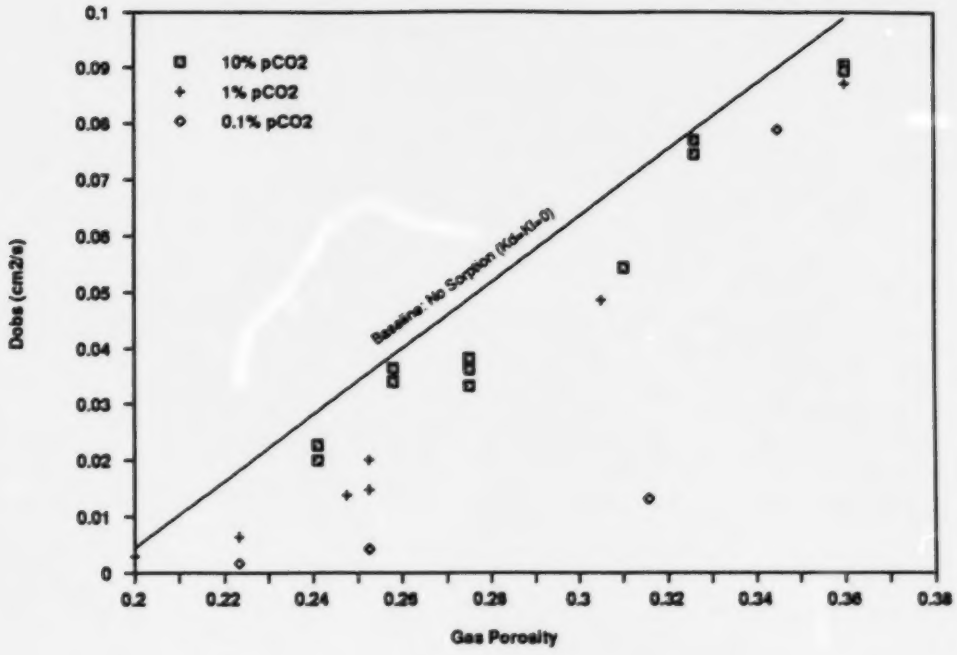

FIGURE 27. Effect of isotopic exchange on measured diffusion coefficients.

Effective diffusion coefficients were estimated using a simple 1-D transport model based on Fick's second law, that is:

$$D_{calc} = D^*_g/R \qquad (2)$$

where R is the retardation factor. For the case of moist silica sand, R took the form of $R = 1 + (n_l/n_g)K1 + (p_b/n_g)Kd.K1$ where the liquid/solid partitioning coefficient was assumed to be negligible (ie, Kd=0). For the dry silica sand, the retardation factor is described by $R = 1+(p_b/n_t)Kd$. The D^*_g values required were calculated from the empirical equation derived from the helium diffusion experiments. Comparison of measured diffusion coefficients D_{obs} to those predicted using eq.(2) showed excellent agreement as indicated by the overall D_{obs}/D_{calc} ratios being near unity (0.957 ± .107) as illustrated in Figure 29. These results indicate that effective diffusion coefficients for $^{14}CO_2(g)$ in partially saturated materials can be estimated quite accurately using a simple "Kd approach" similar to that currently being applied in the prediction of migration rates for ionic solutes in fully saturated systems.

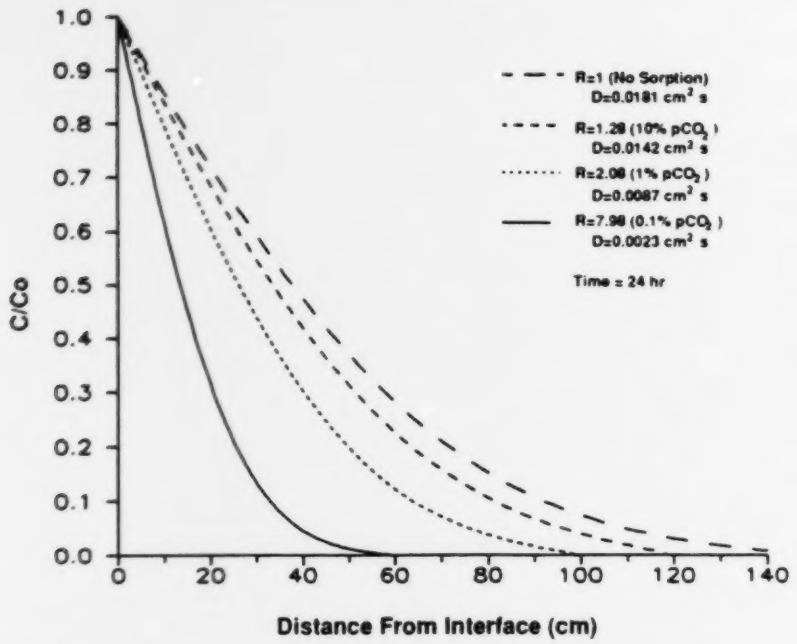

FIGURE 28. Effect of isotope exchange on gaseous C-14 migration.

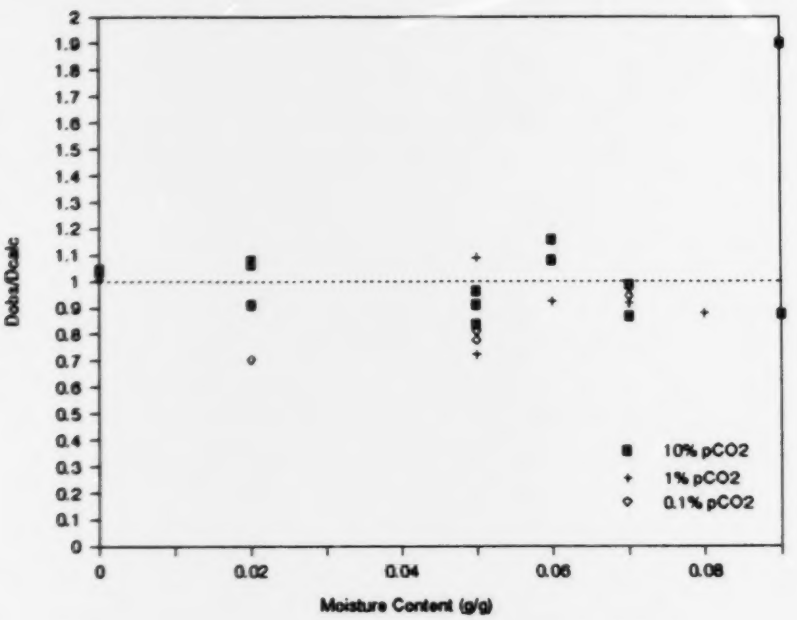

FIGURE 29. Comparison of measured to calculated diffusion coefficients.

2.5 RECRYSTALLIZATION UPTAKE OF C-14 ON CARBONATE MINERALS

Objective and Experimental Approach: The main objective of this study is to evaluate the importance of $CaCO_3$ recrystallization and solid-state diffusion as potential retardation mechanisms for C-14 in natural geologic materials. Laboratory batch experiments are being conducted at a pCO_2 of 1 atm to determine the kinetics and magnitude of $H^{14}CO_3^-$ uptake on calcite mineral grains. The acquired rate constants will be evaluated with respect to their significance to $H^{14}CO_3^-$ migration in groundwater flow systems.

Methods of Investigation: In order to monitor the long-term nature of the C-14 uptake reaction, a closed-system batch cell, capable of monitoring $H^{14}CO_3^-$ uptake by calcite minerals over an extended period of time, was required. This was accomplished by the design and construction of the reaction vessel illustrated in Figure 30. The vessel consists of a 1000 mL Pyrex distilling flask fitted with two threaded Pyrex connector tubes and a side taper joint (19/39). Below the central connector tube a cage was constructed to accommodate a magnetic stir bar, thus ensuring a well mixed solution phase without undue disturbance of the solid mineral phase at the bottom of the vessel. The removable solid teflon plug of the central unit allows easy access to the cage for insertion or removal of the magnetic stir bar while still maintaining a reliable seal once the unit has been tightened.

A volume displacement unit, consisting of a movable glass tube inserted through a teflon bushing/Pyrex connector tube was also added to the reaction vessel. As sampling of the liquid phase proceeds, the glass insert tube of the volume displacement assembly is designed to slide down against a silicon o-ring seal into the reaction vessel. This maintains the integrity of the two phase (liquid and solid) closed system. Sampling will be performed via a 2 mL Pressure-lok syringe inserted through the needle entry port and septum of a Mininert valve in the side taper joint.

Short-term batch experiments (<7 days) are also being conducted using 40 mL glass vials capped with silicon septa. Carbonate saturated solution, traced with $H^{14}CO_3^-$, was used in all of the uptake experiments. The initial set of batch tests was conducted without the addition of calcite to the vials. These tests were designed to determine the extent of C-14 uptake on the vial walls and also to establish if the sampling method would result in significant C-14 loss to the atmosphere. The batch cells were sampled after t=0, t=15 minutes and t=3 days. All experiments were conducted in triplicate. When compared to the C-14 concentrations of the standard solution, no loss of C-14 was observed. This suggests that any loss of C-14 observed during the batch experiments using geologic materials can be directly attributed to solution-solid uptake reactions.

Short-term batch experiments are currently being conducted on samples of acid-leached silica sand and hydrothermal calcite. As with the blank batch tests, the tracer solution consists of $CaCO_3$ saturated water containing C-14 in the form of $H^{14}CO_3^-$ and all tests are conducted in triplicate.

Results: Results of the short-term C-14 uptake experiments conducted on calcite crystals are shown graphically in Figure 31. Although preliminary in nature, Figure 31 shows a two stage uptake reaction similar to that reported by Mozeto (18). During the first stage, uptake appears to follow the standard distribution curve commonly seen in kinetic experiments of trace ionic solutes. That is, an initial increase in the amount of C-14 lost from solution followed by a constant distribution coefficient (Kd) segment. It is anticipated that this stage of C-14 uptake is reversible, however, experiments have not yet been completed to establish this hypothesis.

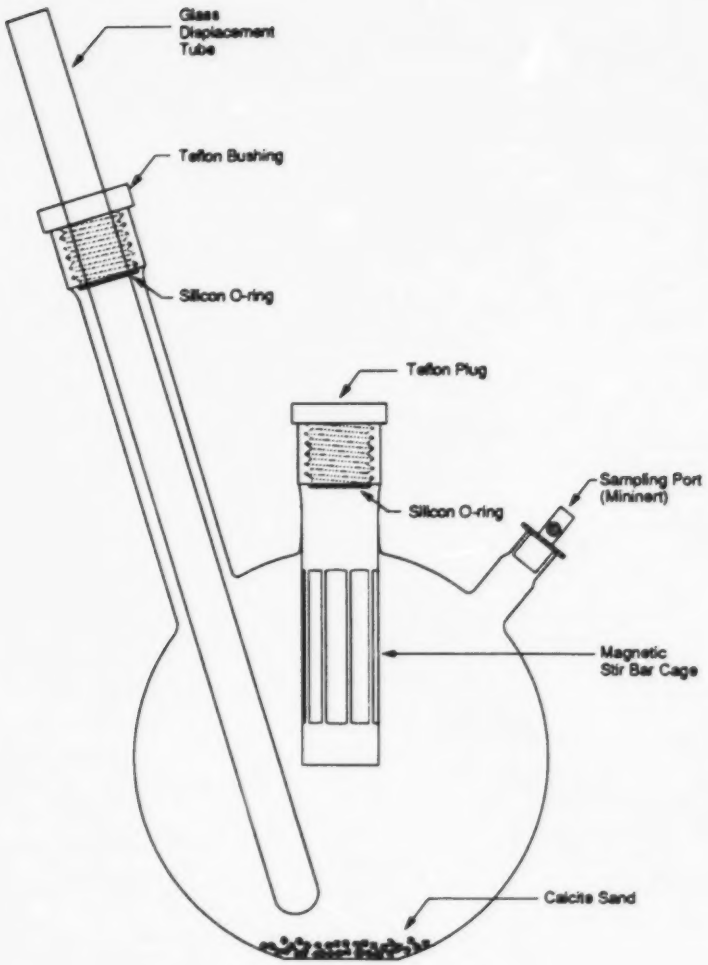

FIGURE 30. Reaction vessel for long-term C-14 equilibrium batch tests.

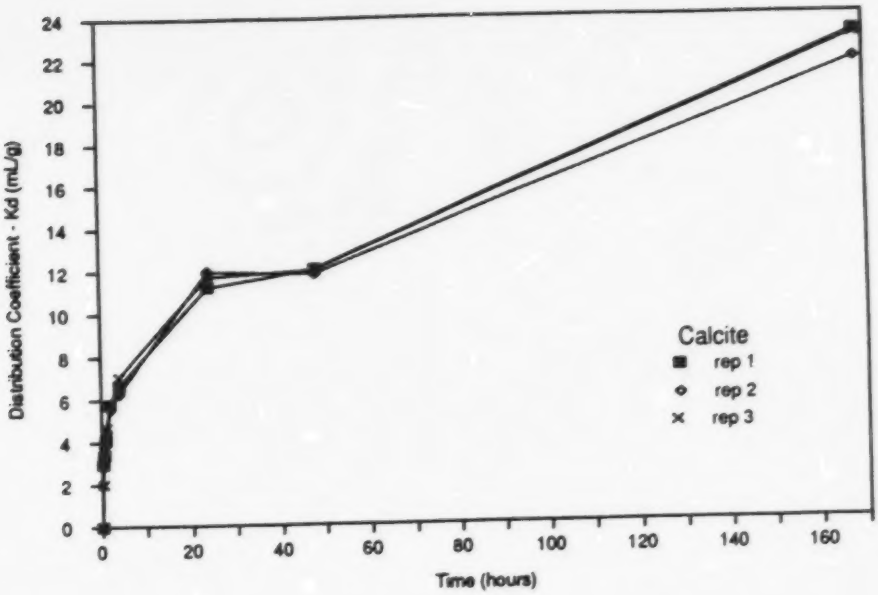

FIGURE 31. Distribution coefficient (Kd) for C-14 versus time, based on equilibrium batch tests for calcite.

The second stage in the uptake process occurred after the 48 hour sampling period and likely represents the influence of C-14 diffusion from the surface of the calcite into the centre of the mineral grain. Results from the long-term uptake experiments will be required in order to quantify the diffusive flux and determine its significance with respect to C-14 transport in natural groundwater systems.

2.6 EVALUATION OF GEOCHEMICAL DATA FROM THE U.S. LOW LEVEL WASTE DISPOSAL SITES

Objective: The purpose of this study is to review and evaluate existing geochemical data from the U.S. radioactive waste disposal sites, such as Maxey Flats in Kentucky, Barnwell in South Carolina, and Sheffield in Illinois, in the context of the establishment of geochemical conditions and processes as related to radionuclide mobility at these sites. Studies of existing low-level radioactive waste disposal sites in the U.S. provide a unique opportunity to investigate the behaviour and fate of radioactive waste nuclides in a natural setting, as well as to evaluate the performance of the waste package under field disposal conditions.

Although the current or future waste packaging and disposal procedures are likely to be much improved from those practiced in the past at the U.S. sites, the in situ observations made at the sites do provide generic information on geochemical factors and processes controlling source term characteristics and radionuclide mobility.

Work Plan: The following areas were considered important in that they shed light on key geochemical factors and processes controlling radionuclide mobility at the sites.

- Exchange and transport of $^{14}CO_2$ in the unsaturated zone at the Sheffield radioactive waste disposal site
- Source term composition of trench leachates from the Maxey Flats radioactive waste disposal site
- Radionuclide migration in sediment cores sampled from contaminated area beneath waste trenches at the Barnwell radioactive waste disposal site

Results and Discussion:

2.61 Exchange and Transport of $^{14}CO_2$ in the Unsaturated Zone at the Sheffield Radioactive Waste Disposal Site

Burial of low-level radioactive wastes in unsaturated glacial and eolian sediments at a waste disposal facility near Sheffield, Illinois, during the period 1967-1978, has resulted in a situation where high partial pressures of $^{14}CO_2$ produced by aerobic decomposition of the waste in the trenches, diffuse through the surrounding unsaturated zone. The nature of the waste was sufficient to give rise to very high $p^{14}CO_2$'s that exceeded atmospheric $^{14}CO_2$ partial pressures by factors greater than 10^6. The resulting gradients in $p^{14}CO_2$ provide a unique opportunity to study the behaviour of $^{14}CO_2$ transport in unsaturated natural geologic materials.

Streigl (19) performed a detailed field and laboratory investigation to study the distribution of $^{14}CO_2(g)$ and other major atmospheric gases in the unsaturated overburden at the Sheffield site. The results, as reported by Streigl, indicated that there was significant retardation to $^{14}CO_2(g)$ migration. Subsequent laboratory uptake experiments on unsaturated materials obtained from the site showed that CO_2 was preferentially adsorbed from gas mixtures, thereby indicating the potential of a large sink for the exchange of $^{14}CO_2(g)$ to the water/sediment phase. The batch experiments were conducted by injection of CO_2, $^{14}CO_2$, and atmospheric gases into an evacuated chamber containing the solid plus pore water phases. This technique does not allow for the determination of isotopic exchange rates alone since the formation of DIC will also occur. Thus the results presented represent total CO_2 uptake (i.e., $^{14}CO_2$ plus $^{12}CO_2$). From these laboratory experiments, Streigl (19) found a strong correlation between CO_2 uptake and the surface area of the sediments; however, differences were evident between the three different types of sediments studied (silt, clayey-silt till, and sandy-silt). The author noted that the influence of mineralogy, particle-size distribution and water content conditions on CO_2 sorption still needs to be quantified.

From the laboratory tests, Streigl further reported that the experimental uptake results of CO_2(total) were from 8 to 17 times larger than was predicted using CO_2-water-calcite thermodynamic constants and that the magnitude of the difference between the CO_2(total) uptake calculated and measured varied with pCO_2. Therefore, experimental adsorption isotherms are required in order to obtain accurate estimates of $^{14}CO_2(g)$ uptake.

Streigl compared the measured field $p^{14}CO_2(g)$ distribution in the unsaturated soil at the disposal site to the distribution simulated by a 2-D finite-difference solution for molecular diffusion. The input parameters were tortuosity, porosity (both water- and air-filled) and a retardation factor describing the dilution of $^{14}CO_2(g)$ due to isotopic exchange with the

inorganic carbon in the water and sediment phases. The numerical results supported the hypothesis that isotopic exchange of gaseous $^{14}CO_2$ into sorbed CO_2 is the primary mechanism for the retardation of $^{14}CO_2(g)$ migration in the unsaturated zone.

2.62 Source Term Composition of Trench Leachates from the Maxey Flats Radioactive Waste Disposal Site

As part of the U.S. Nuclear Regulatory Commission efforts to develop a data base on source term characteristics for the low-level radioactive waste disposal sites in the U.S., a considerable amount of data has been generated on trench leachate geochemistry for the Maxey Flats radioactive waste disposal site, located in Kentucky (20). In addition, the availability of complete chemical data on all leachates sampled from the various waste trenches at Maxey Flats provides an excellent opportunity to evaluate and validate existing geochemical models. In fact, the Maxey Flats trench leachate data are being used for the Commission of European Communities(CEC)-sponsored CHEMVAL/MIRAGE project to evaluate existing geochemical models and their thermodynamic data bases (21).

For the purposes of this report, we will present (a) a synoptic overview of the Maxey Flats source term composition; (b) the oxidation-induced changes in source term geochemistry; and (c) geochemical modeling of reactions likely to take place upon mixing with ambient groundwater or oxidation of anoxic trench leachates.

Results and Discussion: The key features of the source term characteristics for the Maxey Flats disposal site are highlighted below:

A combination of hydrological and geochemical factors determines to a large extent the formation and compositions of the trench leachates. At the Maxey Flats site, the trenches are located in partly weathered illitic shale underlain by unweathered shale having an extremely low hydraulic conductivity. This results in significant water accumulation which is designated as the "bathtub effect". Because of the long residence time of the accumulated water in the trenches, prolonged leaching and microbial degradation of waste materials occur continuously, leading to leachate formation. As a result of such interactions occurring for extended time periods, the resultant trench leachates exhibit significant modifications in terms of inorganic, organic, and radionuclide constituents and acquire geochemical properties that are unique, compared to the ambient groundwater.

The leachates generally exhibit varying degrees of anoxia characterized by negative redox potentials, low dissolved oxygen and sulphate concentrations, high alkalinity, and high ammonia concentrations. The enrichments, to varying degrees, of inorganic, organic, and radionuclide constituents associated with fuel and non-fuel cycle low-level wastes reflect the nature of the leaching process itself and the waste materials. Elevated concentrations of Na^+, K^+, Fe_{total}, Cl^-, dissolved organic and inorganic carbon, and several organic compounds, as well as radionuclides such as ^{3}H, ^{241}Am, ^{60}Co, ^{134}Cs, ^{137}Cs, ^{90}Sr, ^{238}Pu, and $^{239,240}Pu$, are a consequence of waste leaching. Some of the waste-derived organic compounds present in the trenches, such as chelating agents and several carboxylic acids, are strong complexing agents and have the potential to form stable radionuclide complexes and thus enhance nuclide mobility.

In addition to waste leaching and microbial degradation reaction controls on trench leachate compositions, the leachate solutes are also subject to abiogenic precipitation reactions, especially in relatively stagnant systems such as those at Maxey Flats. Solubility calculations based on trench leachate compositions indicate that calcite, dolomite, and rhodochrosite mineral phases

trench leachate compositions indicate that calcite, dolomite, and rhodochrosite mineral phases are likely to form in the trench environments and exert control on the concentrations of Ca^{2+}, Mg^{2+}, Mn^{2+}, and CO_3^{2-}. In the case of iron equilibria, gross supersaturations are found with respect to siderite, mackinawite, amorphous FeS, and pyrite. Some leachates exhibit saturation with respect to vivianite.

Laboratory oxidation experiments were performed to obtain information on the behaviour of anoxic trench leachates as they encounter a less reducing environment along leachate flow paths (22). The results indicate that, upon oxidation, a series of geochemical changes was initiated that results in a drastically different solute chemistry. Some of the important geochemical changes included oxidation of ferrous iron and subsequent precipitation of ferric oxyhyroxide, changes in alkalinity and pH, a drastic increase in Eh, and relatively little change in radionuclide concentrations. The oxidation-induced changes in pH can be interpreted in terms of the competing reactions between the initial buffering capacity of a leachate and the acidity generated as a result of the Fe^{2+} to Fe^{3+} oxidation reaction. Therefore, the buffering capacity and the acid-generating potential of anoxic trench waters are important geochemical controls that maintain a balance between acidity and alkalinity, determining the nature and extent of oxidation-induced changes, as illustrated in Figure 32 for leachates 19s and 27 (22).

As part of Ontario Hydro's formal participation in the CEC MIRAGE 2 CHEMVAL programme of research, this geochemical modelling effort was undertaken to simulate the geochemical changes observed as a result of the oxidation of several anoxic trench leachates, having differing initial buffering capacities. However, in this report, only the modelling results of the oxidation of leachate 19s, a highly buffered system (Table 15), are presented.

Leachate oxidation is achieved by raising the pO_2 of the system. $Fe(OH)_3$(am) or ferric oxyhydroxide is allowed to precipitate at saturation, and, thereafter, the leachate is kept in equilibrium with the solid phase. Assumption of precipitation of ferric oxyhydroxide is reasonable considering that a reddish-brown precipitate was observed during the experiments and that the total dissolved iron decreased with increasing degree of oxidation (22).

The predicted changes in pH and total dissolved iron with increasing degree of oxidation are compared with the laboratory observations (Figure 33). As shown in Figure 33, the modeling predicts all major geochemical changes observed during the leachate oxidation experiments. Leachate 19s is a high alkalinity, well-buffered system, with a large acid-neutralizing capacity. Oxidation of ferrous iron and the subsequent precipitation of ferric oxyhydroxide will generate hydrogen ions and reduce the total alkalinity of the solution. Distinct changes occur at $pO_2=10^{-60}$atm at which the solution reaches saturation with amorphous $Fe(OH)_3$. At this stage, the ferric oxyhydroxide will precipitate out. This is accompanied by a drastic decrease in total iron and alkalinity of the leachate. When oxidation exceeds the point where the redox potential (Eh) equals 200 mV, discrepancies are apparent between observed and modeled pH values. Modeling results indicate that, at this point, more than 99 percent of the initial iron had precipitated and no more dissolved iron is available for reaction. Therefore, both pH and alkalinity should be subject to little changes upon further oxidation. This discrepancy could be a result of the presence of organic carbon in the leachate (430 mg/L dissolved organic carbon) which was not considered in our modeling effort.

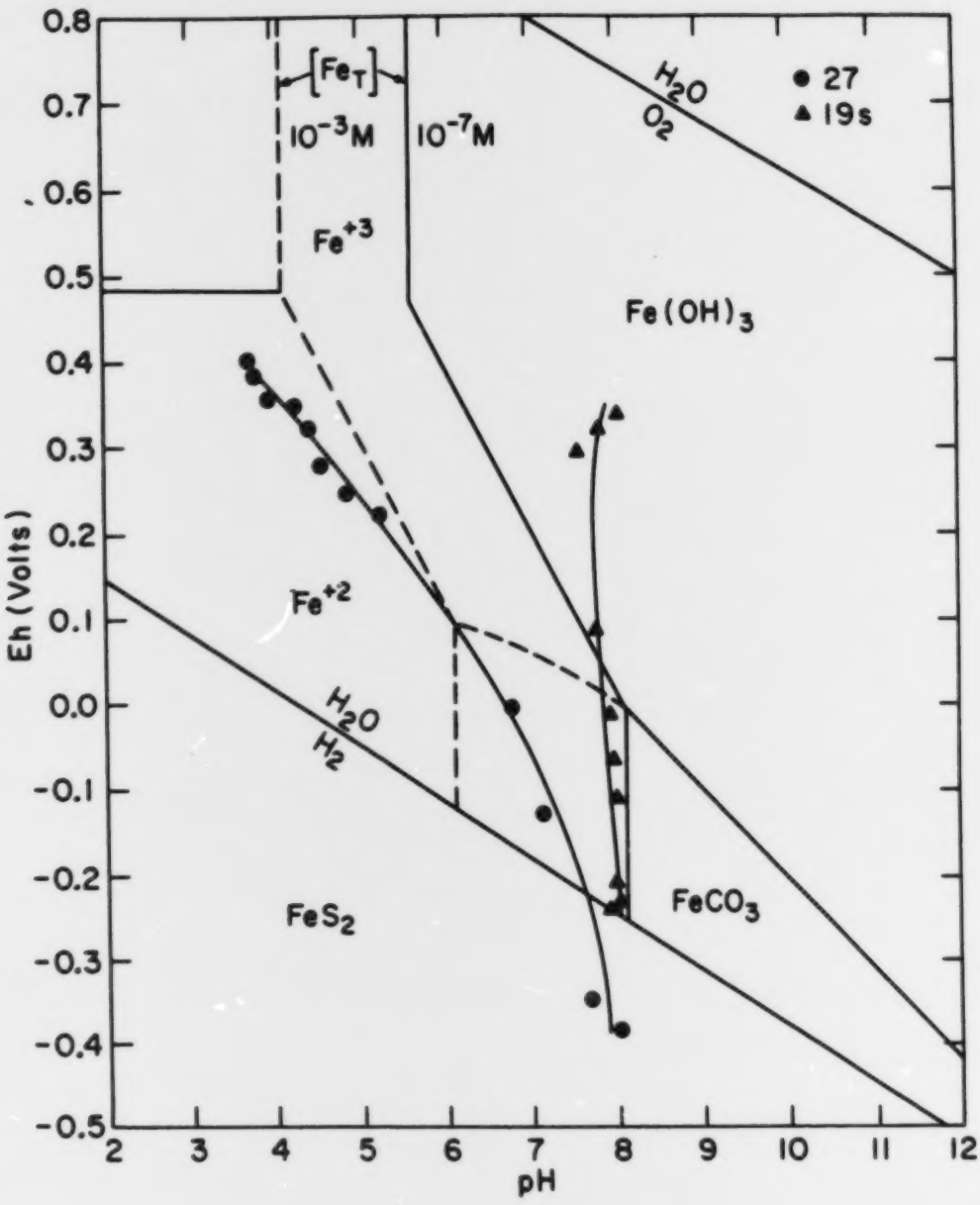

FIGURE 32. The Eh-pH relationships for leachates 27 and 19s depicting different reaction paths and progress during oxidation. Dissolved $\Sigma Fe=10^{-3}M$ to $10^{-7}M$; $\Sigma CO_2=10^{-3}M$; $\Sigma SO_4^{2-}=10^{-4}M$ (22).

Table 15. Chemical Composition of Trench Leachate 19s from the Maxey Flats LLW Disposal Site[a]

Constituents		Concentration (mg/L)
Ca^{2+}		49
Mg^{2+}		128
K^{+}		27
Na^{+}		231
Fe_T		65
Fe^{2+}		62
Mn_T		0.5
Si		b
NH_4^{+}		45
F^{-}		40
Cl^{-}		231
SO_4^{2-}		<2
DIC[c]		170
Alkalinity[d]		1040
pH	7.7	
Eh	-230mV	

[a]From Dayal, et al (22).

[b]Not determined.

[c]Dissolved inorganic carbon.

[d]Reported as $CaCO_3$ (meq/L).

As shown in Figure 34, the degree of saturation for carbonate minerals decreases with progressive oxidation. This is a result of decreasing carbonate content of solution with increasing degree of oxidation. For example, the saturation index for siderite changes from over- to under-saturation, reflecting oxidation of the Fe^{2+} to Fe^{3+} ion accompanied by generation of acidity, which neutralizes the leachate alkalinity (CO_3^{2-}).

The direction and extent of the leachate 19s oxidation reaction progress is best illustrated in the Eh-pH relationship diagram for the Fe-H_2O-S-CO_2 system (Figure 35). The heavy broken line and arrow represent the predicted evolution of leachate chemistry upon incremental oxidation of the solution. The anoxic leachate is initially in the iron sulphide/siderite stability field and, upon progressive oxidation, both the Fe^{2+} and CO_3^{2-} ions are consumed. This contributes to disequilibrium with respect to siderite and finally approaching saturation with respect to ferric oxyhydroxide, as reflected by the final extent of the oxidation reaction progress, based on both observed and predicted changes in leachate chemistry (Figure 35).

The observations made both in the field and laboratory investigations for the Maxey Flats site have important geochemical implications for the modeling of low-level sites in that the source term as an input parameter cannot be assumed to be constant, either spatially or temporally. This is particularly true for anoxic source terms, which can be expected to undergo drastic changes in their chemical character upon oxidation.

Although C-14 was not measured in the trench leachates from the Maxey Flats site, the observations reported above do provide important information on the behaviour of C-14 in the reducing trench environment.

Precipitation of carbonate minerals may serve as an effective sink for carbonate species in the reducing trench environment. In fact, geochemical modeling results show that most Maxey Flats leachates exhibit supersaturation with respect to calcite, dolomite, siderite, and rhodochrosite. The precipitation of these minerals would further remove carbonate, and therefore C-14, from the leachate.

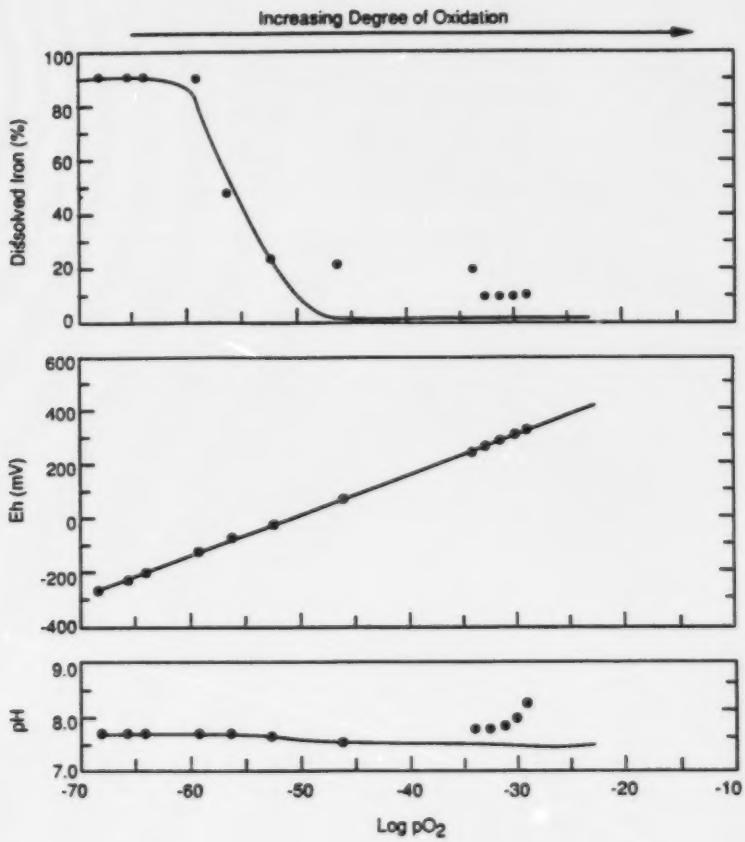

FIGURE 33. Predicted (solid line) and observed (•) changes in anoxic leachate chemistry (19s) with increasing degree of oxidation.

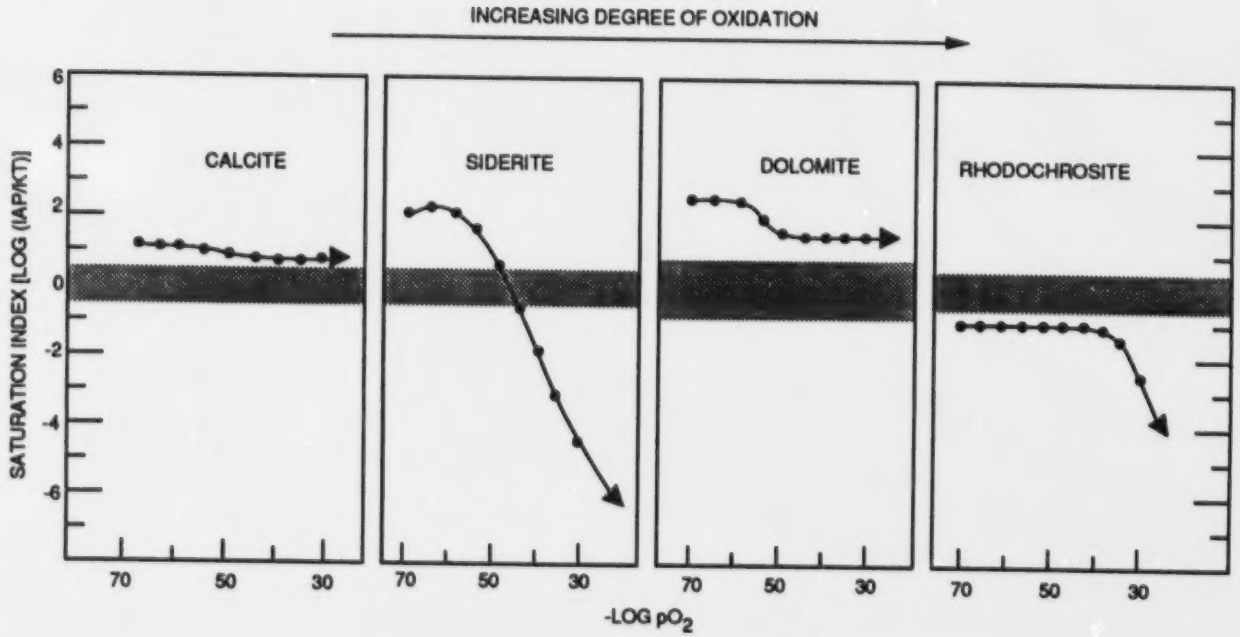

FIGURE 34. Changes in carbonate mineral saturation indices with progressive oxidation of anoxic leachate 19s. Solid lines with arrows indicate the direction and extent of oxidation-induced changes. Shaded areas represent 5% tolerance limits on saturation indices due to uncertainties in the values of mineral solubility products (K_{sp}).

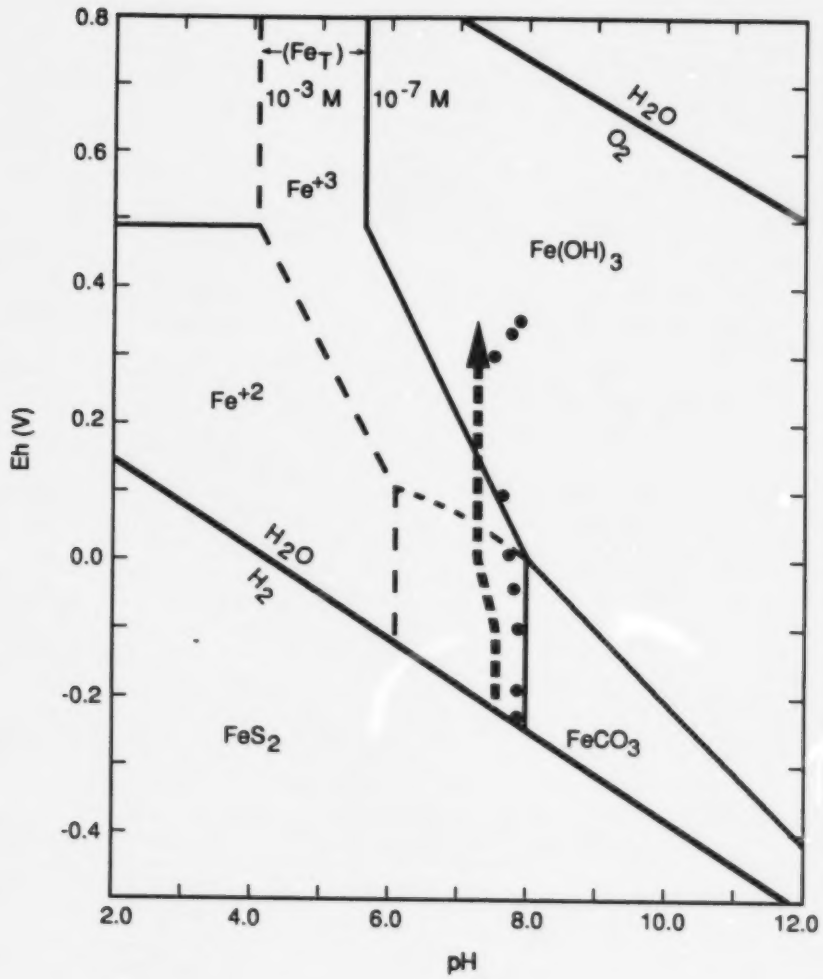

FIGURE 35. THe Eh-pH relationship for leachate 19s reaction path and progress during oxidation. Dissolved $\Sigma Fe = 10^{-3}$M to 10^{-7}M; $\Sigma CO_2 = 10^{-3}$M; $\Sigma SO_4^{2-} = 10^{-4}$M. Both predicted (broken line) and observed (•) changes are illustrated.

A leachate that migrates out of the reducing trench environment will encounter more oxidizing conditions and lower values of pCO_2 as it leaves the zone of active microbial degradation of organic matter and CO_2 and CH_4 production. Since the pCO_2 in the trench environment is much higher than atmospheric, the trench leachate, upon migration to a more oxidizing environment, will encounter pCO_2's closer to atmospheric, resulting in the exsolution of CO_2. Furthermore, the acidity generated as a result of the oxidation of Fe^{2+} to Fe^{3+} in an anoxic leachate will neutralize the initial buffering capacity of the system (dissolved inorganic carbon), thereby resulting in evolution of gaseous CO_2 and, hence, loss of DIC and C-14 from the system.

These are important mechanisms by which C-14 could be lost from the system, and require more attention for consideration in C-14 near-field modeling effort.

2.63 Sediment Core Radionuclide Data from the Barnwell Radioactive Waste Disposal Site

Radionuclide depth profiles are available for several sediment cores taken from contaminated areas underlying the waste disposal trenches at the Barnwell site.

The primary purpose of the study is to evaluate radionuclide mobility at the site, based on in-situ observations. Secondly, the interrelationship between field and laboratory data and observations is important. A considerable amount of radionuclide sorption and migration data (Kd, De) for both reactive and non-reactive radionuclide is available for the Barnwell Hawthorne sediment (23). Predictions of radionuclide migration in the field can be made using the sorption and diffusion data generated in laboratory studies, using the tritium profile to represent unretarded migration. Comparison against actual field observations can then be made to test the validity and applicability of laboratory-derived migration data for predictive purposes. Evaluation of depth profiles for the Pu isotopes, Co-60 and H-3 in selected sediment cores is being carried out.

3.0 CONCLUSIONS

3.1 Cement-Based Backfill Materials Evaluation

Laboratory carbonation tests, performed under accelerated diffusive and advective carbonating conditions, have established that carbonate uptake on grout involves a chemical reaction between CO_2, $_2$ and $Ca(OH)_2$/CSH phases in cement, thereby resulting in the irreversible fixation of CO_3^{2-} in the matrix. The carbonation reaction yields a calcitic end product which is thermodynamically stable and has a high potential to immobilize radiocarbon.

Depending on the initial $Ca(OH)_2$ content of cement, the maximum carbonation capacities of several grout mixes developed at Ontario Hydro range from 15.7 to 19.3% of the mass of the test specimen. However, subsequent tests show that maximum carbonation capacities are not attained for intact test specimens. This is a consequence of the changes induced in material properties, as a result of carbonation.

Some of the important carbonation-induced changes in material properties include, with increasing degree of carbonation, a progressive reduction in porosity, permeability, and average pore-size, and a systematic increase in specific surface area. The observed changes due to carbonation have a beneficial effect on both the radionuclide transport and water ingress properties of the backfill test materials. Reduced permeability and porosity will tend to further minimize water ingress into the disposal system. Reduced water flow will also impede waste leaching and subsequent transport of radionuclides escaping from the waste package.

The consequences of induced carbonation on material transport properties relevant to radiocarbon transport and mobility are also important, considering that the matrix transport parameters tend to control the availability and flux of the reactant to the reaction sites. The induced changes in material properties, as well as the deposition of free water in the matrix interstices generated during the carbonation process, exert a limiting effect on subsequent carbonation of grout, thereby resulting in significantly lower carbonation capacities than calculated or measured (based on pulverized sample) values.

The grout carbonation reaction involves irreversible fixation of CO_3^{2-} (as calcite) in the matrix with the availability and flux of reactant to the reaction sites controlling the rate and extent of carbonate uptake on grout. Preliminary results of additional tests performed to evaluate $^{14}CO_3^{2-}$ uptake on grout also indicate that the final extent of the reaction is dependent on the initial C-14 concentration in solution. This implies that the migration and transport of C-14 in grout backfill cannot be modeled by a simple equilibrium Kd approach.

Furthermore, since the carbonation-induced changes in material properties, as well as the generation of water in the carbonation reaction, tend to impede further carbonation of the grout and, hence C-14 transport, the evolving microstructural changes will have to be taken into consideration in future modeling of C-14 transport in cementitious engineered barriers.

Another important requirement for modeling C-14 transport in grout backfill barriers is the establishment of the lag time for the source term. This is the time between waste emplacement, followed by repository closure, and the onset of actual waste leaching. For a long-lived isotope such as C-14, the lag time may have little effect on the source term itself. However, considering that grout backfill will be subjected to inflow of ambient groundwater containing natural dissolved inorganic carbon, carbonation of grout by inactive carbon could occur during this period. This, to a certain degree, will effectively reduce the overall carbonation capacity of the engineered barrier and, hence affect the relative mobility of C-14.

3.2 Source Term Evaluation for C-14

Preliminary research in the source-term evaluation project has established that the leachant flow rate has a pronounced effect both on the near-field chemistry and the leaching behaviour of C-14. At both static and low flow conditions (0.04 mL/min), the near-field chemistry is dominated by a strongly alkaline environment controlled primarily by portlandite solubility. Under these conditions, no detectable C-14 release is observed. At high flow rate conditions (0.38 mL/min), the near-field pH lies in the range 9.5 to 7.5 and has detectable C-14 concentrations in the leachate, yielding a steady-state incremental leach rate of 2.5×10^{-9}/s. Assuming all C-14 to be present in the form of calcite, the observed C-14 release behaviour can be attributed to the dissolution of calcite, as affected by the near-field pH which, in turn, is determined by the leachant flow rate.

Preliminary findings at Ontario Hydro have important implications with respect to the C-14 reactor waste disposal program in that the near-field chemical environment, brought about by the leaching of grout under stagnant or low flow conditions, would promote the retention of C-14 in the solid phase, thereby contributing to the isolation capacity of the waste form for C-14 for an extended time period. This is particularly important considering that the leaching of cementitious materials in a waste repository, under anticipated low groundwater flow conditions, will result in an alkaline near-field environment which is likely to prevail for time periods commensurate with the half-life of C-14.

Considering that calcite is the host phase for C-14 in cementitious waste forms, further laboratory work is needed to quantify calcite solubility and dissolution rates as a function of varying flow rates and leachant types (BNPD groundwater, deionized water, and cement-equilibrated water). In addition, a quantitative relationship between varying pH and C-14 release needs to be established. The information on this coupled process will be extremely useful for the interpretation of C-14 release behaviour in near-field environments.

3.3 Concrete Materials for High Integrity Containers

Both static and dynamic leaching/dissolution tests were performed on four normal density concretes in deionized water and BNPD groundwater to evaluate their durability in terms of external chemical attack.

The leach data clearly indicate higher leach resistance for test mortars containing silica fume (SF) and/or blast furnace slag (BFS), relative to the control mix (sulphate resistant portland cement - SRPC). Overall, the net effect of the additives, with respect to SRPC, is a significant increase in leach resistance, with BFS being the most effective. Under dynamic leaching conditions, the overall leachability for the test mixes is significantly greater than that observed under static conditions.

Leaching-induced changes in microstructural properties reflect the nature and extent of concrete degradation, with the radial outer zone exhibiting maximal degradation and the inner core remaining relatively unaffected. Considering that test mortars with SF and SF + BFS are the most resistant to external chemical attack under static BNPD groundwater leaching conditions, it can be inferred that these particular concrete materials appear to be the most durable for high integrity containers for the storage/disposal of reactor operating waste at the BNPD site.

Further work is needed in this area to describe and model the degradation of cement due to leaching and groundwater interactions in a waste repository setting. Particular reference should be paid to the current Ontario Hydro concept for storage/disposal of reactor operating waste. Specifically, available geochemical codes could be used to model concrete degradation in terms of the evolving water chemistry and material properties with time. Subsequently, the effects of leaching-induced changes in material microstructural properties on concrete degradation can be assessed. This work will provide important information on the long-term durability of cement-based materials in a repository environment.

3.4 Transport of C-14 in Unsaturated Geologic Materials

A summary of the results and conclusions obtained from equilibrium batch and diffusion experiments conducted on partially saturated silica sand is given below.

$^{14}CO_{2(g)}/^{12}CO_{2(aq)}$ isotopic exchange is diffusion controlled, however, isotopic equilibrium is attained quickly (10 to 15 minutes) indicating that, due to the long time frame considered in pathway analysis, a kinetic term is not required to describe the gas/liquid uptake reaction in transport models.

The magnitude of the gas/liquid uptake reaction is highly pH dependent, with uptake increasing with increasing pH. This suggests that, under pH conditions typical of southern Ontario soils (pH's of 7 to 8), the solution phase could become a substantial sink for gaseous C-14.

Calculated gas-liquid distribution coefficients (Kl) are fairly constant with respect to moisture content. The concept of constant Kl values at variable moisture contents is significant since it would enable retardation factors to be calculated for any moisture content from a single measured distribution coefficient. This would allow the use of a much simpler transport model for contaminant migration predictions.

Measured C-14 concentration profiles obtained from the diffusion experiments were found to be reproducible and exhibited little scatter in the C/Co values with respect to a fitted profile based on Fick's second law. This indicates that $^{14}CO_{2(g)}$ migration in the unsaturated zone can be adequately modelled using Fick's second law of diffusion.

Uptake of C-14 into the solution phase is a significant retardation process, particularly at high water contents. It is anticipated that under conditions typical of southern Ontario soils (higher pH and the presence of solid/liquid exchange reactions on carbonate minerals), the influence of isotopic exchange on C-14 gaseous diffusion will become even more significant and should not be ignored in mathematical transport models.

Comparison of measured to calculated diffusion coefficients showed excellent agreement. These results indicate that effective diffusion coefficients for $^{14}CO_{2(g)}$ can be reliably calculated using an equilibrium distribution coefficient approach, similar to that currently being used to describe the migration of trace ionic species in saturated porous media.

Batch and diffusion experiments should be conducted on materials containing carbonate minerals to evaluate the effect of solid/liquid exchange reactions on effective diffusion coefficients. Since solid-state diffusion of C-14 into the carbonate mineral matrix is a very slow process, quantification of the effect of this uptake on gas-phase migration of C-14 is required. This would entail evaluation of the constant Kd approach for the prediction of gaseous C-14 coefficients where recrystallization upake has occurred.

3.5 Recrystallization Uptake of C-14 on Carbonate Minerals

Results of the short-term C-14 uptake experiments conducted on calcite crystals indicate a two stage uptake reaction. However, results from the long-term uptake experiments will be required to quantify the significance of this process with respect to C-14 transport in natural groundwater systems. Work in this area should be continued to better quantify the diffusion-controlled uptake of C-14, particularly with respect to parameters such as surface area DIC, pH and solution chemistry (ie, effect of other ions such as Mg, Ca etc, on C-14 uptake).

3.6 Evaluation of Geochemical Data from the U.S. Low-Level Radioactive Waste Disposal Sites

Existing geochemical data from the U.S. radioactive waste disposal sites, such as Maxey Flats in Kentucky, Barnwell in South Carolina, and Sheffield in Illinois are being evaluated in the context of the establishment of geochemical conditions and processes as related to radionuclide mobility at these sites. The following areas were considered important in that they shed light on key geochemical factors and processes controlling radionuclide mobility at the sites.

- Exchange and transport of $^{14}CO_2$ in the unsaturated zone at the Sheffield radioactive waste disposal site
- Source-term composition of trench leachates from the Maxey Flats radioactive waste disposal site
- Radionuclide migration rates in sediment cores sampled from contaminated area beneath waste trenches at the Barnwell radioactive waste disposal site

Sheffield Radioactive Waste Site

Burial of low-level radioactive wastes in unsaturated glacial and eolian sediments at a waste disposal facility near Sheffield, Illinois during the period 1967 - 1978 has resulted in a situation where high partial pressures of $^{14}CO_2$ produced by aerobic decomposition of the waste in the trenches cause C-14 to diffuse through the surrounding unsaturated zone. The resulting gradients in $p^{14}CO_2$ provide a unique opportunity to study the in-situ behaviour of $^{14}CO_2$ transport in unsaturated natural geologic materials.

The results of a detailed field and laboratory investigation to study the distribution of $^{14}CO_2(g)$ and other major atmospheric gases in the unsaturated overburden at the Sheffield site indicated that there was significant retardation to $^{14}CO_2(g)$ migration. Subsequent laboratory uptake experiments on unsaturated materials obtained from the site showed that CO_2 was preferentially adsorbed from gas mixtures, thereby indicating the potential of a large sink for the exchange of $^{14}CO_2(g)$ to the water/sediment phase.

Comparison of the measured field $p^{14}CO_2(g)$ distribution in the unsaturated soil at the disposal site to the distribution simulated by a 2-D finite-difference solution for molecular diffusion supported the hypothesis that isotopic exchange of gaseous $^{14}CO_2$ into sorbed CO_2 is the primary mechanism for the retardation of $^{14}CO_2(g)$ migration in the unsaturated zone.

Maxey Flats Radioactive Waste Site

A combination of hydrological and geochemical factors determines to a large extent the formation and compositions of the trench leachates. The leachates show significant modifications in terms of inorganic, organic, and radionuclide constituents and acquire geochemical properties that are unique compared to the ambient groundwater chemistry.

The leachates generally exhibit varying degrees of anoxia that is characterized by negative redox potentials, low dissolved oxygen and sulphate concentrations, high alkalinity, and high ammonia concentrations. The enrichments, to varying degrees, of inorganic, organic, and radionuclide constituents associated with fuel and non-fuel cycle low-level wastes reflect the nature of the leaching process itself and the waste materials. Elevated concentrations of Na^+, K^+, Fe_{total}, Cl^-, dissolved organic and inorganic carbon, and several organic compounds as well as radionuclides such as ^{3}H, ^{241}Am, ^{60}Co, ^{134}Cs, ^{137}Cs, ^{90}Sr, ^{238}Pu, and $^{239,240}Pu$, are a consequence of waste leaching. Some of the waste-derived organic compounds present in the trenches, such as chelating agents and several carboxylic acids, are strong complexing agents and have the potential to form stable radionuclide complexes and thus enhance nuclide mobility.

In addition to waste leaching and microbial degradation reaction controls on trench leachate compositions, the leachate solutes are also subject to abiogenic precipitation reactions, especially in relatively stagnant systems such as those at Maxey Flats.

As part of Ontario Hydro's formal participation in the CEC MIRAGE 2 CHEMVAL programme of research, a geochemical modelling effort was undertaken to simulate the geochemical changes observed as a result of the oxidation of several anoxic trench leachates, having differing initial buffering capacities. The modeling results for leachate 19s (a high alkalinity, well-buffered system with a large acid-neutralizing capacity) indicate that all major geochemical changes observed during the leachate oxidation experiments can be accurately predicted. Oxidation-induced changes observed for other trench leachates are also being modeled.

The observations made both in the field and laboratory investigations for the Maxey Flats site have important geochemical implications for the modeling of low-level sites in that the source term, as an input parameter, cannot be assumed to be constant, either spatially or temporally. This is particularly true for anoxic source terms which can be expected to undergo drastic changes in their chemical character upon oxidation.

Although C-14 was not measured in the trench leachates from the Maxey Flats site, the observations reported above do provide important information on the behaviour of C-14 in the reducing trench environment. For example, precipitation of carbonate minerals may serve as an effective sink for carbonate species in a reducing environment. In fact, geochemical modelling results show that most Maxey Flats leachates exhibit supersaturation with respect to calcite, dolomite, siderite, and rhodochrosite. The precipitation of these minerals would further remove carbonate, and therefore C-14, from the leachate.

A leachate that migrates out of the reducing trench environment will encounter more oxidizing conditions and lower values of pCO_2 as it leaves the zone of active microbial degradation of organic matter and subsequent CO_2 and CH_4 production. Since the pCO_2 in the trench environment is much higher than atmospheric, the trench leachate, upon migration to a more oxidizing environment, will encounter lower pCO_2's, resulting in the exsolution of CO_2.

Furthermore, the acidity generated as a result of the oxidation of Fe^{2+} to Fe^{3+} in an anoxic leachate will neutralize the initial buffering capacity of the system (dissolved inorganic carbon), thereby resulting in evolution of gaseous CO_2 and, hence, loss of DIC and C-14 from the system.

These are important mechanisms by which C-14 could be lost from the system, and require more attention for consideration in C-14 near-field modelling effort.

Barnwell Radioactive Waste Site

Depth profiles for the Pu isotopes, Co-60 and H-3 in sediment cores taken from beneath two waste trenches at the Barnwell site are being interpreted to evaluate radionuclide mobility at the site, based on in situ observations. The main aim of this study is to compare calculated radionuclide migration rates based on laboratory-derived radionuclide sorption and diffusion data, against actual field observations so that the validity and applicability of laboratory-derived migration data for predictive purposes can be assessed.

4.0 ACKNOWLEDGMENTS

The authors would like to thank Mr. R. Klein, Mr. D. Wilmot, and Ms. K. Eagleson for conducting the laboratory analysis and data reduction. We are also grateful to summer students Ms. E. Vander Damm (University of Waterloo) and Mr. D. Flynn (Queen's University) for their assistance in the laboratory. The expertise and assistance provided by the Concrete Technology Section in preparation of the concrete and grout test specimens is gratefully acknowledged.

Funding for these projects was provided jointly by the Nuclear Engineering Department and the Civil Research Department.

Approved by:

T.W. Klym
Manager
Civil Research Department

Submitted by:

R. Dayal
Program Coordinator
Rock Sciences Section

H.M. Johnston
Hydrogeologist
Rock Sciences Section

Reviewed by:

A.T. Jakubick
Supervising Engineer
Rock Sciences Section

Z. Zhou
Engineer
Rock Sciences Section

RD/HMJ/ZZ:at

REFERENCES

1. Drolet, T.S., Stewart, W.B., and Lo, K.K., "Nuclear Reactor Wastes: Development Considerations for a Conditioning Program for Long-Term Storage or Disposal. In: Waste Management and Fuel Cycles '78, R.G. Post (ed.), 1979.

2. Nott, B.R., "Determination of Carbon-14 in Spent Ion Exchange Resins". Inter. Jour. Applied Radiation Isotopes, 33, 584-585, 1982.

3. Isaac, H.N. and Rao, P.K.M., "Management of Low and Intermediate Level Nuclear Wastes at Ontario Hydro." Presented at the International Symposium on Alternative Low Level Waste Technologies, Illinois, Chicago, 1986.

4. Rao, P.K.M., "Long Term Management Requirements for Low and Intermediate Level Radioactive Wastes from CANDU Nuclear Generating Stations". Design and Development Division - Generation, Ontario Hydro Report No 88-262, 1988.

5. Russell, S.B., "Assessing Low and Intermediate Level Radioactive Waste Disposal - 1987 Progress Report". Design and Development - Generation, Ontario Hydro Report No. 87-533, 1987.

6. Allen, R.E., "Management of C-14 Waste - Background for 1988 Vault Modeling Studies". Design and Development Division - Generation, Ontario Hydro Report No. 88-222, 1988.

7. Moddle, P.M. and Reardon, E.J., "Evaluation of the Efficiency and Chemistry of Reactions Between Cementitious Grout and Carbon Dioxide". Final Report, University of Waterloo Research Institute, University of Waterloo, 1986.

8. Reardon, E.J., James, B.R., and Abouchar, J., "Geochemical Aspects of the Carbonation of Grout: I. High Pressure Carbonation of Cementitious Grout". Final Report, University of Waterloo Research Institute, University of Waterloo, 1987.

9. Reardon, E.J. and Abouchar, J.A., "Geochemical Aspects of the Carbonation of Grout: II. Reactions Between Carbonate-Form Exchange Resins and a Grout Slurry". Final Report, University of Waterloo Research Institute, University of Waterloo, 1987.

10. Dayal, R. and Klein, R., "Evaluation of Cement-Based Backfill Materials". Ontario Hydro Research Division Report No. 87-223-K, 1987.

11. Dayal, R. and Klein, R., "CO_2/Grout Interactions and Their Relevance to C-14 Attenuation in Cementitious Backfill Materials". Radiochimica Acta, 44/45, 263-270, 1988.

12. Dewaele, P.J. and Reardon, E.J., "Chemical Characteristics of the Carbonation of Grout". Final Report, University of Waterloo Research Institute, University of Waterloo, 1989.

13. Hespe, E.D., "Leach Testing of Immobilized Radioactive Waste Solids - A Proposal for a Standard Method". Atomic Energy Review, 9, 195-207, 1971.

14. Chou, L., Garrels, R.M., and Wollast, R., "Comparative Study of the Kinetics and Mechanisms of Dissolution of Carbonate Minerals". Paper Presented at the International Congress of Geochemistry and Cosmochemistry, Paris, France, 1988.

15. Plummer, L.N., Wigley, T.M.L., and Parkhurst, D.L., "The Kinetics of Calcite Dissolution in CO_2-Water Systems at 5° to 60° and 0.0 to 1.0 atm. CO_2. Amer. Jour. Sci, 278, 179-216, 1978.

16. Atkinston, A. "The Time-Dependence of the pH Within a Repository for Radioactive Waste Disposal". AERE Report, AERE-R 11777, 1985.

17. Hooton, R.D., "Permeability and Pore Structure of Cement Pastes Containing Fly Ash, Slag, and Silica Fume". Proc. ASTM C-1 Symp. on Blended Cements, 128-143, 1985.

18. Mozeto, A.A., Fritz, D., and Reardon, E.J., "Experimental Observation on Carbon Isotope Exchange in Carbonate-Water Systems". Geochim. Cosmochim. Acta, 48, 495-504, 1984.

19. Striegl, R.G., "Exchange and Transport of $^{14}CO_2$ in the Unsaturated Zone. Ph.D. Dissertation, The University of Wisconsin, 1988, 149 p.

20. Dayal, R., Pietrzak, R.F., and Clinton, J.H., "Geochemical Investigations at the Maxey Flats Radioactive Waste Disposal Site". Topical Report. Brookhaven National Laboratory, BNL-NUREG-51820, NUREG/CR-3993, 1984.

21. Read, D. and Broyd, T.W., "The CHEMVAL Project: Status Report, 1989". Presented at a Plenary Meeting of the CEC MIRAGE Project Co-ordinating Group, Brussels, 1989.

22. Dayal, R., Pietrzak, R.F., and Clinton, J.H., "Oxidation-Induced Geochemical Changes in Trench Leachates from the Maxey Flats Low-Level Radioactive Waste Disposal Site". Nuclear Technology, 72, 184-193, 1986.

23. Dayal, R., "Source Term Studies at Shallow Land Burial Sites". Progress Report, Brookhaven National Laboratory, BNL-NUREG-34332, 1984.

APPENDIX I

ontario hydro
research division

To: Dr. T.W. Klym
Manager
Civil Research Department

REACTOR OPERATING WASTE DISPOSAL PROGRAM

L. Konecny/R.D. Hooton

1.0 INTRODUCTION

This report summarizes the investigation of physical properties and microstructural characteristics carried out on a series of four sanded cement grouts.

The grouts were prepared as part of the program to evaluate concretes as High Integrity Container (HIC) Materials. Samples were also cast for use in diffusion and leaching experiments by H. Johnston and R. Dayal.

2.0 MIX PROPORTIONS

The mix proportions of the four trial grouts are given in Table 1. Mortar specimens were made in order that the sand would provide volume stability for the various tests to be performed on them. Standard Ottawa silica sand was used in a 2.75:1.0 ratio by mass of cement. Mortars were mixed according to ASTM C 305 using a melamine formaldehyde condensate superplasticizer to obtain flow values of 100 to 115%. Mix #13871 was a control mix with CSA Type 50 (T50) portland cement. Mix #13872 had 10% replacement by volume of cement by silica fume (SF) similar to AECL reference grout. Mix #13873 had 15% silica fume replacement because it was thought that the extra silica fume would further enhance the physical properties.

Mix #13874 had both 10% silica fume and 30% blast furnace slag (BFS) by volume replacements similar to high-strength concretes developed for use in Scotia Plaza building in Toronto. (The BFS usually enhances later age properties.) All mixes were prepared at a water to cementing materials ratio (w/cm) of 0.35.

job	file	date	report no.
44-318-462	841.2	February 20, 1989	S89-4-K

3.0 RESULTS

3.1 Compressive Strength

Compressive strength results are presented in Table 1. The highest compressive strength values at all ages (except 3 days) were recorded for specimens made from mixes #13872 and #13873 with 10% and 15% replacement levels of cement by silica fume, respectively . At 365 days, mix #13874 (10% SF + 30% BFS) displayed similar strength to that of mix #13872; however, this mix displayed the lowest strength values at early ages. This is caused by the fact that the pozzolanic reaction between $Ca(OH)_2$ (liberated during hydration of C_3S and C_2S) and BFS is a much slower process than that between Ca(OH) and SF. The lowest compressive strength at the age of 365 days was that of the control mix (#13871).

3.2 Porosity

Porosities were determined by the mercury intrusion technique and the results are presented in Table 2. Mortars with 10% and 15% SF showed lower total porosities (volume of pores down to 18 Å radius as measured by mercury intrusion porosimetery on samples dried at 100°C) than that of the control mix or the mix with SF and BFS.

Since the water permeability of mortars is governed by the volume of capillary pores present rather than by total porosity, the volumes of pores larger than 500 Å radius are also tabulated. Here, the mortar with 10% SF replacement displayed the lowest porosity at 365 days; therefore, this mortar is likely to be the least permeable.

3.3 Chloride Permeability

The permeability in this program was measured by the AASHTO T277 Rapid Chloride Permeability Technique. The electrical charges passed through the specimens during 6 hour period are shown in Table 2. Classification of chloride permeability according to Whiting (1981) is presented in Table 3. From the results presented in Table 2, it follows that the chloride permeability of the control mortar at 365 days is classified as high and the permeabilities of the remaining mortars are classified as very low.

Submitted by:

L. Konecny

L. Konecny
Engineer
Concrete Technology Section

Reviewed by:

R.D. Hooton
Engineer
Concrete Technology Section

LK:cmf/mao

TABLE 1

MIX PROPORTIONS AND COMPRESSIVE STRENGTH RESULTS

Mix #	13871	13872	13873	13874
Mix: (Volume % replacement)	T50	T50/10%SF	T50/15%SF	T50/10%SF/30%BFS
(Mass % replacement)	T50	T50/7.2%SF	T50/11%SF	T50/7.3%SF/29.4BFS
w/cm	0.35	0.35	0.35	0.35
Flow %	109	106	105	105
Melment Dose ml/g cm	180/5530	110/5860	125/5280	128/5240
ml/kg cm	32.5	20.5	23.7	24.4
Average Compressive Strength: [MPa]				
3 days (2)*	31.9	36.0	31.7	19.4
7 days (8)	39.0	45.2	42.6	33.6
28 days (3)	47.5	60.7	62.0	54.6
91 days (3)	48.4	67.6	64.7	57.1
182 days (2)	52.2	64.7	66.6	60.4
365 days (3)	57.2	66.0	71.6	65.6

Note: T50 - CSA Type 50 Portland cement
SF - Silica fume
BSF - Blast furnace slag
cm - Cementing materials
* - number of specimens tested

TABLE 2

POROSITY AND CHLORIDE PERMEABILITY RESULTS

Mix #	13871	13872	13873	13874
Mercury Intrusion Porosimetry: [% by volume of specimen]				
Total Porosity >18 Å Radius:				
7 days	15.3	13.3	13.8	15.9
28 days	15.3	12.6	12.9	12.7
91 days	11.3	10.6	11.4	11.6
182 days	11.4	10.0	10.0	11.1
365 days	12.2	10.6	11.0	11.5
Porosity > 500 Å Radius:				
7 days	4.9	4.0	4.5	4.7
28 days	5.0	3.5	4.2	3.7
91 days	4.5	3.2	4.5	3.7
182 days	4.0	3.0	3.4	3.9
365 days	4.6	3.4	4.0	4.0
Chloride Permeability: (Coulombs)				
7 days	>9060*	1995	1220	1120
28 days	>8640**	480	275	300
91 days	6250	425	250	255
268 days	4863	517	313	281
365 days	4027	575	341	309

* 255 min
** 313 min

TABLE 3

INTERPRETATION OF CHLORIDE PERMEABILITY
FROM CHARGE PASSED (WHITING, 1981)

Chloride Permeability	Charge Passed (Coulombs)	Type of Concrete
High	4,000	High water-cement ratios (0.6)
Moderate	2,000-4,000	Moderate water-cement ratio (0.4-0.5)
Low	1,000-2,000	Low water-cement ratios "Iowa" dense concrete
Very Low	100-1,000	Latex modified concrete Internally sealed concrete
Negligible	100	Polymer impregnated concrete Polymer concrete

Whiting, D., "Rapid Determination of the Chloride Permeability of Concrete," Report Prepared for Federal Highway Administration, Washington, D.C., by Construction Technology Laboratories, a Division of PCA, Skokie, Ill., August 1981.